

On the Numerical Simulation of Activated Processes

John E. Straub

Submitted in partial fulfillment of the
requirements for the degree
of Doctor of Philosophy
in the Graduate School of Arts and Sciences.

COLUMBIA UNIVERSITY

1987

Abstract

On the Numerical Simulation of Activated Rate Processes

John Edward Straub

Here we describe a new method for evaluating rate constants for activated processes using numerical simulation – the absorbing boundary method. While approximate, this method is shown to be accurate and faster than previously existing methods. It is applied to several distinct physical systems. Rate constants for a one-dimensional non-Markovian system with exponential friction are calculated and shown to deviate from theoretical predictions. A qualitative analysis of trajectories gives a physical explanation for the deviations and indicates what an accurate theory must include. Also, rate constants for a two-dimensional Markovian system are calculated and used to test the validity of two conflicting predictions for the rate of energy activation. A useful criterion is proposed for determining the regions of validity of each theory. Finally, a theory for the calculation of non-adiabatic effects in activated barrier crossing is presented. We compare our theory with recent simulation results and find excellent agreement.

Contents

1	Introduction	1
2	A Summary of Rate Theories	7
2.1	Transition State Theory	7
2.2	Energy Diffusion	8
2.3	Spatial Diffusion	14
2.4	Connection Formulas	16
3	The Absorbing Boundary Method	17
3.1	Background	17
3.2	An Approximate Method	20
3.3	Numerical Results	25
3.4	Discussion	28
4	One-dimensional Non-Markovian Systems	31
4.1	The Model	31
4.2	Numerical Results	33
4.3	Discussion	37
5	Two-dimensional Markovian Systems	42
5.1	The Problem	42
5.2	A Model System	45
5.3	Simulation Results	46
5.4	Adiabatic Elimination	50

5.5	Eigenvalue Analysis	52
5.6	External Noise and Energy Transfer	56
5.6.1	Resonance Streaming	59
5.6.2	Surface Crossing	59
5.6.3	Resonance Diffusion	60
5.7	Discussion	61
6	Non-Adiabatic Transitions	66
6.1	The Model of Cline and Wolynes	67
6.2	Our Theory	71
6.3	Comparison	77
6.4	Discussion	79
7	Conclusion	81
7.1	Is Transition State Theory Enough?	81
7.2	Biomolecular Systems	82
7.3	Small Molecules and Models	84
	References	86
	Appendix	94

We have physicists, geometricians, chemists,
astronomers, poets, musicians and painters in
plenty, but we have no longer a citizen among us.

Jean Jacques Rousseau

Acknowledgments

My four years in New York, at Columbia, have been more than fun. In this time I have had the opportunity to learn and reason with the finest people I have met in my life. I first thank my advisor, Bruce Berne, for his unending patience and encouragement. Few know him, at their loss, as a founding father of the student senate, or one who tolerated the endless mantras of Allen Ginsberg as an anti-war demonstrator in Washington, DC. I respect him as a fine scientist as well as an individual of character and conscience.

Millard Alexander, with whom I worked as an undergraduate and to whom I owe much, impressed upon me the importance of one's fellow students in graduate school, saying that he had learned more science from them than any other source. I was particularly fortunate then to find myself in a class of seven other theoretical students in my first year. Two soon left, but five have lasted – Mike Borkovec, Jane Budimir, Dave Hsu, Leslie Root, and Anders Wallqvist – and it has been a pleasure to share this small space which is the ninth floor with them.

In particular, I benefited greatly from my time spent with Mike Borkovec. Much of what I think a chemist should be comes from watching Mike do so well what I did with such mediocrity. I thank Leslie Root for attending many forums on animal rights, which I sponsored along with my good friend Avi Magidoff;¹ attending such events is the true test of an open mind, as animal rights was, and remains, the avant-avant-garde.

I thank Anders Wallqvist for being my buddy, traveling with me from the now defunct 8BC Club to the slightly safer Nicaragua during the fifth anniversary of their revolution in July 1984, and for introducing me to Dr. Hunter S. Thompson. We have learned from *Pink* what Ezra Pound and John Hinckley have in common, as well as who killed John Belushi. I have always promised him that things would get better, and with most thanks to Peggy I think they finally have.

I have spent more time with my roommate and companion Dave Hsu than with anyone else in my time here. I could not have asked for a more understanding friend. Together we have been arrested² and seen Billy Bragg. Somewhat more importantly, we have read, listened to, and learned from linguist and political critic Noam Chomsky. To expose oneself to Noam

¹Here, I give Avi the credit that *The Spectator* never did, as the initiator of actions against the College of Physicians and Surgeons which eventually led to the exposure of their violation of NIH Guidelines and a suspension of funding.

²We were expressing our opposition to the trade embargo of Nicaragua in May 1985. Later, we were vindicated while the embargo continues until this day. The irony is that we were guilty of disorderly conduct while the Nicaraguan government was in violation of no aspect of international law.

Chomsky is, I believe, to sense what it is like to think clearly.³

I must thank Howie Alper for his endless humor, which could get as raw as was required, and our countless discussions on psychology; in particular, our merciless criticism of a misguided group of ill-meaning individuals – the behaviorists. I collectively thank three post-docs I have known, Dev Thirumalai, Dave Coker, and Amy Bug, for the enthusiasm and energy they brought to the floor and our famed Berne-group meetings. Frank Johnston, I thank for thinking rigorously, and for sticking it out.

I also thank Glenn Martyna for presenting to our otherwise democratic floor his unique brand of Reaganism. To Joe Bauer, thanks for providing us with a less frightening alternative.

I also wish to honor those who have sacrificed their careers in chemistry so that they might earn enormous salaries – Eric Bruskin, Sam Collins, Doug Garrity, and Jack Bartholomew. I enjoyed their company while they were with us.

Jim Skinner I thank for the great special topics course he taught in my first year, and for making the yearly canoe trips something to fear. I thank Phil Pechukas for being a reasonable and entertaining chairman, and for once defending my character from an unkindly bunch Uptown, who shall, after careful consideration, remain anonymous.

³“It is the responsibility of intellectuals to speak the truth and to expose lies.” That is a “truism” which Noam Chomsky, more than anyone I know, believes in and lives by. The fact that his work is consistently suppressed in the major media is a crime of incomparable measure. I refer you to the thesis of David Ambrose Hsu, Columbia University (1986) for useful citations of Noam Chomsky’s recent work.

Finally, I thank my parents, who have provided me with most of my aforesaid character, and my wife-to-be-on-July-11th Mary Beth Sharp who has been a constant source of support, love, and understanding.⁴

⁴In addition, she introduced me to my favorite writer, José Ortega y Gasset, by presenting me with a 25¢ copy of *The Mission of the University*.

To live is to feel oneself lost – he who accepts
it has already begun to find himself.

José Ortega y Gasset

Vitae

John Edward Straub was born in Denver, Colorado on April 11, 1960, the only child of Jack Sydney and Maurine Butler Straub. He subsequently lived in Kansas City, Kansas; Detroit, Michigan; and Richmond, Virginia before moving to New Orleans, Louisiana where he attended De La Salle High School, graduating in 1978.

He began his undergraduate studies as a pre-veterinary student at Louisiana State University in Baton Rouge before transferring to the University of Maryland at College Park. There he worked with Millard Alexander, graduating with honors in chemistry in 1982. Since that time, he has studied under Bruce Berne at Columbia University. He is a recipient of the Pegram Award and the Graduate Teaching Award. After graduation, he will continue his studies with Martin Karplus at Harvard University as a National Institutes of Health Postdoctoral Fellow.

To my parents

1 Introduction

The theory of activated processes has been a central area of chemical research for decades. Early work concentrated on the activated crossing of a barrier separating metastable reactant and product states. Complicated, and usually unknown, multidimensional potential surfaces were approximated by a single reaction coordinate (Fig. 1). Bistability often arose from the crossing of two bound state electronic surfaces and the process of electronic surface crossing was assumed to be adiabatic. The simplest models neglected solvent interactions. A bimolecular reaction then consists of gaseous particles colliding with some frequency and energy distribution determined by their mass, temperature, and density. The rate is determined by the number of collisions per unit time multiplied by the fraction of particles which have an energy exceeding the activation energy[67].

When solvent is included, the situation appears, at first, more complicated. It is, however, made substantially simpler by transition state theory, first proposed by Eyring[36] and Wigner[114], which is based on two clear and often excellent approximations[83]. First, it is assumed that the reactant states are in thermal equilibrium such that there is an equilibrium distribution of states at all energies up to and including the activation energy. Second, those particles which are activated will move, on average, with their equilibrium velocity across the barrier top without collision, and become stabilized product. In this way, the process of barrier crossing can be thought of as an activation step for gaining the barrier energy followed by

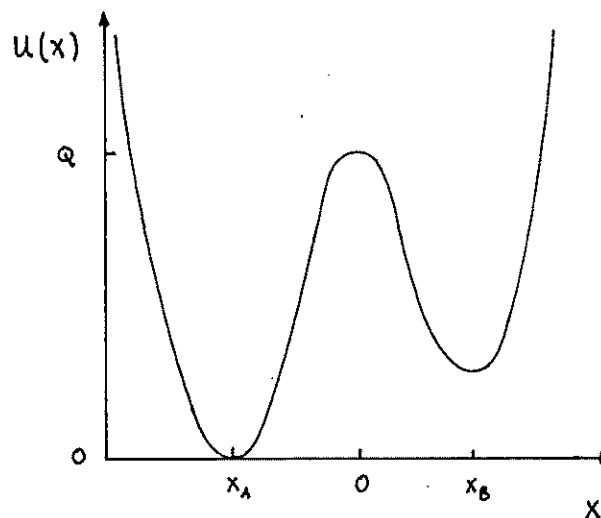


Figure 1: Typical potential separating reactants from products.

crossing of the barrier region. It is easy to understand that the transition state theory gives the maximum possible equilibrium rate constant.

Much work has been done to understand how to calculate the best transition state theory rate constant[105] as well as to extend the idea of system and solvent to include solvent dissipation effects important in barrier crossing[85]. *The two assumptions of transition state theory, and the study of their validity, now form the central area of research on activated processes.*

Smoluchowski set the style for future work by calculating the bimolecular recombination rate constant for particles randomly diffusing in a constant potential[100]. He modeled the two reacting particles as random walkers whose positional probability distribution satisfies a diffusion equation. In this way, he was able to calculate the rate for recombination as a function of the viscosity or diffusion coefficient for the solvated particle. Extensions

were later made by Onsager[81], and Debye[30] who included Coulombic interaction and hard core repulsion.

It was Kramers who first applied the ideas of diffusion controlled reactions in the context of measuring deviations from transition state theory, using the Markovian Langevin equation[62]. He looked at the limits of low and high friction, or collision rate, where the rate limiting steps are energy activation and spatial diffusion across the barrier region, respectively. In the case of low friction, he found that the rate for energy activation increases linearly with the friction. For high friction, the rate for spatial diffusion across the barrier region was found to decrease in proportion to the inverse friction. It followed that the total rate constant begins at zero for zero friction, increases linearly with increasing friction, reaches a maximum, at or below the transition state value, and then decreases as the friction increases further. A summary of much of this work, along with recent work extending these ideas to more realistic models, is presented in Chapter 2.

Physical experiments have recently shown the existence of the Kramers' turnover, the maximum in the rate as a function of the solvent pressure or viscosity, for stilbene photoisomerization on an excited electronic state surface[68,37,64] and halogen recombination reactions[82,51]. When varying the solvent density, it is important to assess the importance of equilibrium solvent effects in the form of the potential of mean force, which can affect the barrier height and the well and barrier frequencies[94]. In the case of photoisomerization, charges are present and variation in the solvent polarity

must be accounted for when examining the rate for viscosity dependence. Such a situation has been examined by Hicks and coworkers[50].

Due to the complicated nature of real reaction systems, skepticism is particularly important when interpreting results. For example, examine the history of our understanding of the chair boat isomerization of cyclohexane which was first studied by Jonas and coworkers[49] at high pressure and later by True and coworkers at lower pressures[92,93]. It has long been used as an experimental example of spatial diffusion; it exhibits a decreasing rate constant as a function of pressure at high pressures. Zawadzki and Hynes further analyzed this system and proposed that the Kramers' turnover may actually occur in the gas phase, at far lower pressures than was indicated by experiment[118]. However, the recent work of Singer, Kuharski and Chandler[96] predicts that the transition state normalized rate increases with pressure over the whole density range, indicating that in the experimentally studied pressure range the rate may be limited by energy activation.

Because of the difficulty in applying theoretical ideas to experimental results, numerical simulation plays a particularly important role. Molecular dynamics[5,86] and Monte Carlo[72] techniques have revolutionized the study of the liquid state. However, there is an inherent difficulty in studying activated processes, that is that they require *activation*. For an activation barrier of energy Q , the fraction of states which are activated will be proportional to $e^{-\beta Q}$ where $\beta = 1/k_B T$. Therefore, for large barriers, many trajectories must be followed to examine only a few activated events.

This difficulty was circumvented by the pioneering work of Keck and others[116,7,11,60]. Following their ideas, Chandler formulated the reactive flux method for calculating activated rate constants[28]. The beauty of this method is that all trajectories begin at the transition state and therefore all simulated trajectories are, themselves, activated. The reactive flux method has been applied to a number of liquid state reaction systems for both stochastic[56] and realistic[6] solvent models as well as reactions at surfaces[3].

While the reactive flux method is a vast improvement over the straightforward simulation method, for systems with many degrees of freedom calculation of the rate constant often proves to be infeasible. In Chapter 3 we present an approximate version of the reactive flux, the absorbing boundary method, which is highly accurate and often orders of magnitude faster.

Much work has been done to extend the ideas of Kramers to more realistic models of the solvent and reaction system[54], as well as to propose connection formulas which provide a rate constant valid for all friction[112]. Hynes and coworkers used the non-Markovian generalized Langevin equation to model the finite time relaxation of the solvent[78,39,40], while Skinner and Wolynes studied various collision models as well as connection formulas for bridging between the low and high friction regimes to provide a rate constant valid for all friction, or collision rate[98,97]. In Chapter 4 we present simulation results for the reaction rate of a one-dimensional non-Markovian system

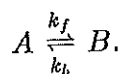
over a wide range of friction. The simulation results are used to investigate the range of validity of connection formulas for non-Markovian systems.

More recent work has concentrated on treating multidimensional reaction systems[22,14]. Current and excellent reviews exist discussing these developments[54,44,17]. In Chapter 5 we present numerical results for a two-dimensional Markovian system where the data is used to examine the validity of multidimensional energy activation theories.

Finally, Wolynes and coworkers have recently initiated the study of the effects of non-adiabatic curve crossing on activated barrier crossing. This work is particularly important to the study of electron transfer in biomolecules such as hemoproteins. In Chapter 6 we propose a statistical theory which combines the Landau-Zener-Stueckelberg theory [29] with the absorbing boundary formalism (Chapt. 3). We compare our predictions with recent numerical simulation data [57] and find excellent agreement.

2 A Summary of Rate Theories

Here we present a summary of existing theories for the calculation of reaction rate constants. These results will be referred to in the chapters which follow. Unless otherwise stated, all rate constants discussed will apply to a reaction system consisting of two metastable states, wells A and B, where



The total rate constant $k = k_f + k_b$ where k_f and k_b are the forward and backward rate constants.

2.1 Transition State Theory

The transition state theory rate is defined as[15]

$$k_{TST} = \frac{\langle \dot{x} \delta(x) \theta(\dot{x}) \rangle}{X_A X_B} \quad (2.1)$$

where $x = 0$ defines the transition state surface, $\theta(\dot{x})$ is the Heaviside step function which is 1 for $\dot{x} > 0$ and 0 otherwise, $\langle \dots \rangle$ indicates a canonical average with partition function $Q = \int d\Gamma \exp(-\beta H(\Gamma))$, $H(\Gamma)$ is the Hamiltonian for the reacting system, and X_A and X_B are the equilibrium mole fractions for the reactant and product wells, respectively. Thus, k_{TST} is simply the equilibrium flux across the transition state surface assuming that i) a constant thermal population of reactant states exists in the well with energy Q and ii) all activated particles cross the transition state surface and are trapped in the product well. If the reactant well and saddle are assumed

harmonic, then in the limit of high barriers, $\beta Q \gg 1$, one may use the approximate formula[99]

$$k_{TST} = \frac{1}{\pi} \frac{\prod_{i=1}^N \omega_i^{(W)}}{\prod_{i=2}^N \omega_i^{(S)}} e^{-\beta Q}, \quad (2.2)$$

where $\omega_i^{(S)}$ are the non-reactive normal mode frequencies of the saddle while $\omega_i^{(W)}$ are normal mode frequencies of the reactant well.

2.2 Energy Diffusion

In an experimental system, collisions between the solvent molecules and the reaction coordinate extend over a finite period of time and are continuous in force and time. If the reduced mass of the reacting coordinate greatly exceeds the mass of the solvent molecules, there will be a separation of time scales whereby each collision between a solvent molecule and the reaction coordinate may be approximated by a force extending over an infinitesimal period of time; successive collisions can be assumed continuous in occurrence and uncorrelated in force, i.e., the force is Markovian. These assumptions lead to weak collision models which are often formulated using the one-dimensional Langevin equation

$$\ddot{x} = -\frac{\partial V(x)}{\partial x} - \gamma \dot{x} + R(t) \quad (2.3)$$

where x is the system variable (which may represent the internuclear separation of two reacting atoms or the dihedral angle of an isomerizing molecule); $V(x)$ is the internal potential experienced by x , γ is the damping coefficient, and $R(t)$ is the fluctuating force representing all other coordinates which are

not treated explicitly. The fluctuating force and damping coefficient satisfy the second fluctuation dissipation theorem

$$\langle R(0)R(t) \rangle = 2k_B T \gamma \delta(t) \quad (2.4)$$

which requires $R(t)$ to be a white noise which fluctuates such that the average thermal energy of the bath is $k_B T$. It is usually assumed that $R(t)$ is a Gaussian stochastic process. Eqs.(2.3) and (2.4) rest on the assumption that the bath coordinates relax very quickly compared to the system variable so that motion of the system is uncorrelated with that of the bath.

Kramers[62] used Eq.(2.3) to calculate rate constants for the escape of a particle from a well in the presence of a thermal bath. He looked at two limiting cases, the underdamped limit where γ is very small and the rate limiting process is energy activation in the well, and the overdamped limit where γ is very large and the rate limiting process is spatial diffusion across the barrier top.

In the underdamped limit, γ is small and the probability that a particle will gain energy much greater than $k_B T$ is unlikely. However, once the particle is activated, having enough energy to cross the barrier top, it will feel little damping and be able to oscillate freely and leave the reactant well. In the case of a symmetric double well potential for large energy barriers $Q \gg k_B T$, where the well is approximated by a harmonic oscillator, the rate constant for energy activation is given by

$$k_{ED} \sim \frac{1}{2} \beta Q \gamma e^{-\beta Q} \quad (2.5)$$

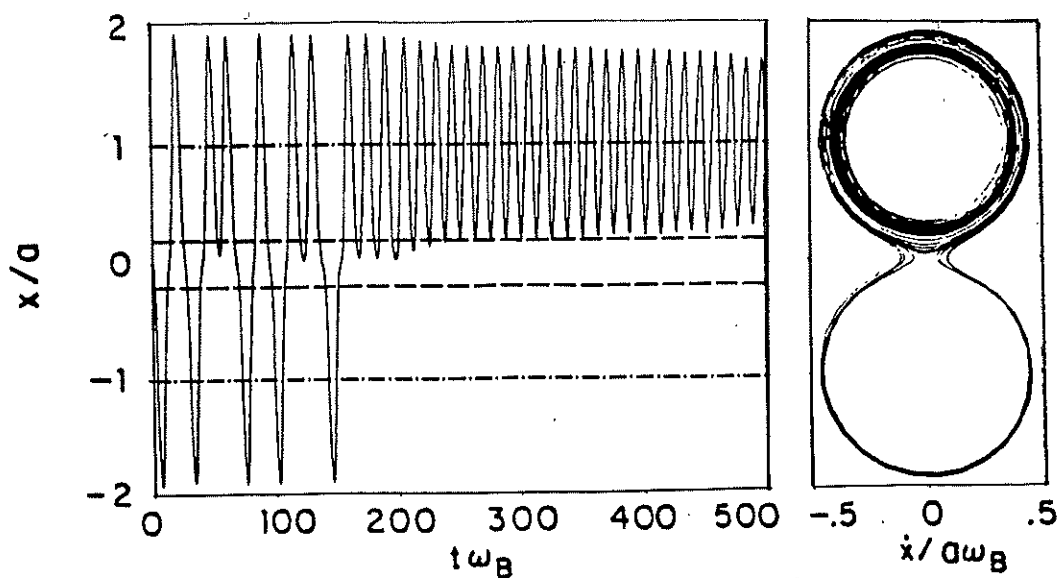


Figure 2: Typical trajectory in the energy diffusion regime. $x = \pm a$ are the positions of the well minima while ω_B is the harmonic barrier frequency.

where the factor of $\frac{1}{2}$ indicates that once the particle is activated it will oscillate many times before being trapped and have equal probability of being trapped in either well. A typical trajectory in the energy diffusion regime for a one-dimensional bistable potential is shown in Fig. 2. Notice the inertial motion of the excited trajectory leads to recrossings of the barrier region before deactivation. In addition, the first few oscillations show that energy is lost and gained due to the fluctuating force leading to intermittent trapping in one well followed by crossing of the barrier region.

The two most obvious limitations of the Kramers' model are i) $x(t)$ is a Markov process so that memory effects one might expect in a condensed phase are neglected and ii) Eq.(2.3) is one-dimensional so that systems which have degrees of freedom strongly coupled to the reaction coordinate are

not accurately treated. Recent work has extended the result of Eq.(2.5) to both one-dimensional non-Markovian systems[40] and Markovian[22] and non-Markovian[117] systems of many dimensions. We summarize these results below.

To include memory effects Grote and Hynes used the non-Markovian generalized Langevin equation[55,4,39]

$$\ddot{x} = -\frac{\partial V(x)}{\partial x} - \int_0^t dt' \zeta(t-t') \dot{x}(t') + R(t) \quad (2.6)$$

where $\zeta(t)$ is a time-dependent friction kernel and $R(t)$ is the fluctuating force which satisfies the second fluctuation dissipation theorem

$$\langle R(0)R(t) \rangle = k_B T \zeta(t). \quad (2.7)$$

Eq.(2.4) is a special case of Eq.(2.7) where $\zeta(t) = 2\gamma\delta(t)$. The generalized Langevin equation removes the assumption of a mass, or timescale, separation between the reaction coordinate and the solvent. This allows for a more realistic treatment of correlated collisions between solvent molecules and the reaction coordinate. The force exerted by the solvent on the reaction coordinate is non-Markovian. With a proper choice of time dependent friction kernel $\zeta(t)$ one may include both short time collisional dynamics and long time hydrodynamic effects. However, individual collisions are not separated in time or force so that the generalized Langevin equation is, like the Langevin equation, a weak collision model.

For the case of a one-dimensional symmetric double well potential, with energy barrier $Q \gg k_B T$, the rate for energy activation is given by[40]

$$k_{ED} = \frac{1}{2} \left[\int_0^Q dE \frac{e^{\beta E} \omega(E)}{D(E)} \int_0^E dE' \frac{e^{-\beta E'}}{\omega(E')} \right]^{-1} \quad (2.8)$$

where $\omega(E)$ is the oscillator frequency at energy E and $D(E)$ is the energy diffusion coefficient. If the well may be assumed harmonic to a good approximation[40]

$$k_{ED} \sim \frac{1}{2} \beta Q \operatorname{Re} \hat{\zeta}(-i\omega_0) e^{-\beta Q} \quad (2.9)$$

where $\operatorname{Re} \hat{\zeta}(-i\omega_0)$ is the real part of the Fourier transform of $\zeta(t)$ taken at the well frequency ω_0 . This result is exactly Eq.(2.5) where the constant damping term γ has been replaced by the friction felt by a particle moving at the frequency of the well.

To treat many dimensional systems in the Markovian limit Borkovec and Berne used the multidimensional Langevin equation

$$\ddot{\mathbf{x}} = -\nabla V(\mathbf{x}) - \gamma \cdot \dot{\mathbf{x}} + \mathbf{R}(t) \quad (2.10)$$

which is the obvious generalization of Eq.(2.3) to more dimensions. They took an N -dimensional system consisting of a bistable reaction coordinate linearly coupled to $N - 1$ non-reactive coordinates where the coupling is such that equipartitioning of the energy between the N degrees of freedom is fast compared to the rate for activation in the well and the full phase space is

chaotic. If the energy barrier $Q \gg k_B T$, in the harmonic approximation the rate for energy activation is found to be[22]

$$k_{ED} \sim \frac{1}{2} \frac{(\beta Q)^N}{N!} \sum_{i=1}^N \gamma_{ii} e^{-\beta Q} \quad (2.11)$$

where γ_{ii} is the i th diagonal element of the friction tensor γ . For $N = 1$, Eq.(2.11) reproduces the one-dimensional result of Eq.(2.5). The fundamental difference between the higher dimensional result and the one-dimensional result of Eq.(2.5) is that the prefactor in Eq.(2.11) depends strongly on the dimension of the system. The factor $(\beta Q)^N/N!$ comes from the density of states for the N -dimensional harmonic well. This indicates that as the number of states in the well at energy Q increases so does the probability of reaching that total energy. A result similar to Eq.(2.11) has been found for multidimensional non-Markovian systems[117].

The generalized Langevin equation models the solvent interaction with the reaction coordinate using a continuous time random force. An alternative dynamic description is given by the impulsive collision models. In these impulsive models, each collision is separate in time and force. Hence, impulsive collision models are sometimes referred to as strong collision models as opposed to the weak collision models discussed above. The most popular is the BGK model which assumes that the reaction coordinate velocity is randomized, according to a Maxwell distribution, on each collision, where collision times are randomly sampled from a Poisson distribution[19]. Skinner and Wolynes solved the rate at which a particle, whose dynamics correspond to

the BGK model, escapes from a harmonic well[98]. For a symmetric double well potential, the rate for energy activation is given approximately by

$$k_{EA} \sim \frac{1}{2} \alpha [e^{-\beta Q} - \text{erfc}(\sqrt{\beta Q})/2] \quad (2.12)$$

where α is the collision frequency and $\text{erfc}(x)$ is the complementary error function[2].

2.3 Spatial Diffusion

For large damping and any non-Markovian friction kernel the rate for saddle crossing was first solved by Grote and Hynes[39]. They chose to model the system using the generalized Langevin equation (Eq.(2.6)). Unable to calculate the first passage time from one well minimum to another, following Kramers[62] they approximated the potential in the barrier region as an inverted parabola with frequency ω_B and assumed a steady state distribution outside the barrier region. They obtained the rate constant[39,41] which has since been derived in a number of different formulations[46,85] and contexts[44,115,45,84]. It is given by

$$k_{GH} = k_{TST} \frac{\lambda}{\omega_B} \quad (2.13)$$

λ is the largest positive root of the Grote-Hynes relation

$$\lambda^2 + \lambda \tilde{\zeta}(\lambda) = \omega_B^2 \quad (2.14)$$

where $\tilde{\zeta}(s)$ is the Laplace transform of the friction on the reaction coordinate per unit mass. k_{TST} is the transition state result applied to the one-dimensional reaction coordinate.

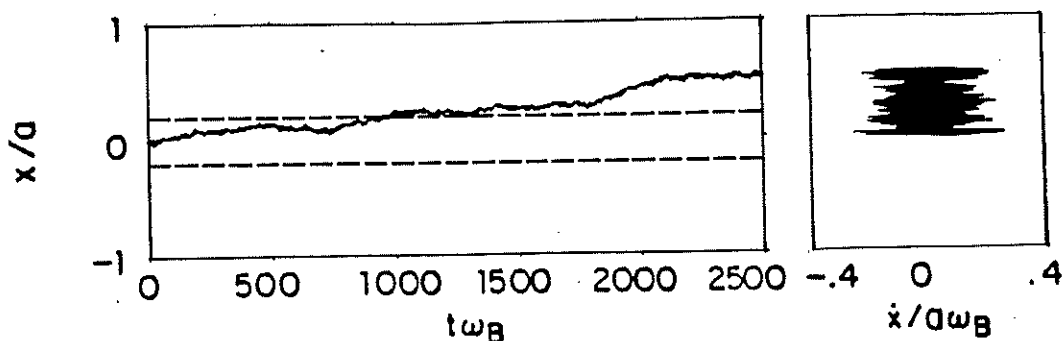


Figure 3: Typical trajectory in the spatial diffusion regime. $x = \pm a$ are the positions of the well minima while ω_B is the harmonic barrier frequency.

If the solvent relaxes quickly, the friction can be approximated as the zero frequency value γ and the Grote-Hynes rate reduces to the Kramers result[62]

$$k_{GH} = k_{TST} \frac{[\omega_B^2 + (\gamma/2)^2]^{1/2} - \gamma/2}{\omega_B} \quad (2.15)$$

which reduces to transition state theory for $\gamma = 0$ and varies inversely with the friction at large γ as the Smoluchowski rate constant[100]

$$k_{GH} \sim k_{TST}(\omega_B/\gamma). \quad (2.16)$$

A typical trajectory in the overdamped, spatial diffusion regime for a one-dimensional bistable potential is shown in Fig. 3. Notice that the trajectory performs a random walk in the barrier region while losing energy and slowly drifting into the well.

Alternatively, for a cusped barrier where $\omega_B \gg \omega_0$, which is common in reactions involving electronic curve crossing[106], the spatial diffusion rate is

given by[62]

$$k_{SD} \sim k_{TST}(\omega_0/\gamma)(\pi\beta Q)^{\frac{1}{2}}. \quad (2.17)$$

The Grote-Hynes theory has been applied to a wealth of chemical systems; there exist excellent reviews summarizing this work[53,54].

2.4 Connection Formulas

To define the total rate constant, k , for all friction we use the connection formula[117,39,46,47]

$$k^{-1} \simeq k_{ED}^{-1} + k_{GH}^{-1} \quad (2.18)$$

where k_{ED} is the appropriate energy diffusion rate, and k_{GH} is the Grote-Hynes rate constant for crossing the saddle[117,39,41,32,46,47]. Similar ideas have led to more complicated rate formulas which give similar results[98,26].

3 The Absorbing Boundary Method

The absorbing boundary method, which uses molecular dynamics to determine rate constants for activated barrier crossing, is discussed. This method requires much less CPU time than the straightforward simulation of the reactive flux in the low and high friction regimes. When applied to the Langevin equation the absorbing boundary method gives excellent agreement with the results of Kramers' theory.⁵

3.1 Background

There are many instances in chemistry and physics where it is important to simulate reactions



involving a transition between stable species separated by an energy barrier. If the activation energy Q is large compared to $k_B T$, barrier crossing is infrequent and a straightforward computer simulation will result in too few barrier crossings to allow determination of the rate constant. To avoid this problem one calculates the reactive flux[116,60,7,11,28]

$$\hat{k}(t) = \frac{\langle \dot{x} \delta(x) \theta[x(t)] \rangle}{\langle \dot{x} \delta(x) \theta(\dot{x}) \rangle} \quad (3.2)$$

where $\langle \dots \rangle$ indicates a canonical or microcanonical average, x is the reaction coordinate, $x = 0$ is the position of the transition state surface, and $\theta(x)$ is

⁵Much of the material presented in this chapter appears in J.E.Straub and B.J.Berne, *J. Chem. Phys.*, 83:1138, (1985) and J.E.Straub, D.A.Hsu and B.J.Berne, *J. Phys. Chem.*, 89:5188, (1985).

the Heaviside step function; $\theta[x(t)]$ is unity if the system at time t is to the right of the transition state (that is, in well B).

If $Q \gg k_B T$, $\hat{k}(t)$ will decay on two widely different time scales[28]. There will be a fast transient decay from the initial value, followed by a very slow decay

$$\hat{k}(t) \rightarrow \kappa e^{-(k_f+k_b)t} \quad (3.3)$$

where k_f and k_b are the forward and backward rate constants and κ is the "plateau value" of the reactive flux or the dynamical transmission coefficient

$$\kappa = \frac{k_f + k_b}{(k_f + k_b)_{TST}} \equiv \frac{k}{k_{TST}} \quad (3.4)$$

where $k = k_f + k_b$ is the exact kinetic rate constant, and $k_{TST} = (k_f + k_b)_{TST}$ is the transition state theory approximation to k (Chap. 2).

It is possible to express the reactive flux in a form more useful for the purpose of computer simulation[18]

$$\begin{aligned} \hat{k}(t) &= \int d\Gamma [P^{(+)}(\Gamma) - P^{(-)}(\Gamma)] \theta[x(t)] \\ &= \langle \theta[x(t)] \rangle_+ - \langle \theta[x(t)] \rangle_- \end{aligned} \quad (3.5)$$

where

$$P^{(\pm)}(\Gamma) = \frac{\dot{x}\theta(\pm\dot{x})\delta(x)e^{-\beta H(\Gamma)}}{\int d\Gamma \dot{x}\theta(\pm\dot{x})\delta(x)e^{-\beta H(\Gamma)}} \quad (3.6)$$

are normalized phase space distribution functions. To calculate $\hat{k}(t)$ one samples points in phase space from these distribution functions, and runs molecular dynamics trajectories for each of the sampled points[56,90,3] (see Appendix). The delta function implies that all trajectories begin at $t =$

0 at $x = 0$; that is, at the transition state. In the $P^{(+)}(\Gamma)$ distribution, the velocity \dot{x} is positive and the system starts out moving towards well B, whereas in $P^{(-)}(\Gamma)$, \dot{x} is negative and the system moves towards well A. It follows that $\langle \theta[x(t)] \rangle_+$ and $\langle \theta[x(t)] \rangle_-$ are the fractions of sampled trajectories which are in well B at time t given that at time $t = 0$ they were at $x = 0$ and the initial velocity is either $\dot{x} > 0$ or $\dot{x} < 0$, respectively.

Thus to simulate a reacting system[109,87,91] one may use Monte Carlo techniques to sample initial states from $P^{(\pm)}(\Gamma)$ and molecular dynamics to calculate $\hat{k}(t)$ using Eq.(3.5). This procedure requires following a large number of trajectories for a sufficiently long time to determine κ . To determine $k = k_f + k_b$ from κ , a separate Monte Carlo simulation is required to determine the transition state theory rate constant (Chap.2) which may be written as the flux correlation function Eq.(2.1) [28,18]. In such a case, one samples values for the position and velocity using the Monte Carlo algorithm [72] and the distribution $\delta(x)\dot{x}e^{-\beta H(\Gamma)}$ where x is the reaction coordinate constrained to the transition state. In Cartesian coordinates, the velocity and position may be sampled independently[21] and

$$k_{TST} = \frac{1}{2X_A X_B} \langle |\dot{x}| \rangle S(0) \quad (3.7)$$

where $S(0) = \langle \delta(x) \rangle$ is the probability of finding the reaction coordinate at the transition state $x = 0$ [15]. Alternatively, one could follow the trajectories for a very long time and thereby determine the exponential decay of $\hat{k}(t)$ (see Eq.(3.2)); however, this requires considerable computer time. Since all

trajectories needed to determine κ originate at the top of the barrier, the reactive flux method avoids the need for trajectories to be activated.

The reactive flux approach requires much less computer time than other methods. It has been used to simulate reactions in the liquid state[56,90,3]. Nevertheless, for very small or very large friction, the trajectories may recross the transition state many times before they are trapped and even the reactive flux becomes very costly in CPU time.

3.2 An Approximate Method

Here we describe an approximate method in which the initial states are sampled according to $P^{(\pm)}(\Gamma)$ after which each trajectory is computed only until it is absorbed by an "absorbing boundary" at the transition state. This method allows determination of κ as well as k and k_{TST} and requires much less CPU time than does the full reactive flux calculation, outlined above, when applied to very low and very high friction regimes, i.e., when there are large deviations from the transition state rate constant. Its accuracy is demonstrated by applying it to a simulation of one-dimensional Langevin dynamics in a symmetric double well. The resulting rate constant as a function of the friction constant agrees with Kramers' theoretical predictions over a very wide density range. We also compare the full time dependence of the reactive flux in a two-dimensional system with that determined by the absorbing boundary method. The agreement is very good and the method agrees with both the transition state rate and the real rate constants.

For simplicity, consider a symmetric double well potential with wells A and B (see Fig. 1). Let $P(t-t')$ be the fraction of trajectories which at time t' are at the transition state ($x=0$) moving towards well B ($\dot{x} > 0$) and by time t have not yet recrossed $x=0$. The flux crossing $x=0$ for the first time is then $j(t-t') = -\partial_t P(t-t')$. If it is assumed that on recrossing the barrier the distribution of particles at the transition state is given by $P^{(\pm)}(\Gamma)$, then the population of particles that recross the transition state at time t' which have not recrossed a second time by time t is just $P(t-t')$. If we assume that on every recrossing the distribution of particles at the transition state is $P^{(\pm)}(\Gamma)$, then $\langle \theta[x(t)] \rangle_+$ can (thanks to Dave Hsu) be expressed in terms of $P(t)$ and $j(t)$ as

$$\begin{aligned} \langle \theta[x(t)] \rangle_+ &= P(t) + \int_0^t dt_2 \int_0^{t_2} dt_1 P(t-t_2) j(t_2-t_1) j(t_1) \\ &+ \int_0^t dt_4 \int_0^{t_4} dt_3 \int_0^{t_3} dt_2 \int_0^{t_2} dt_1 P(t-t_4) j(t_4-t_3) \\ &\times j(t_3-t_2) j(t_2-t_1) j(t_1) + \dots \end{aligned} \quad (3.8)$$

The first term on the right represents the fraction of trajectories still in B at time t . The second term represents the fraction of trajectories that have crossed once from B to A, then crossed back to B and been trapped. The quantity $j(t_1)dt_1$ is the fraction of trajectories crossing for the first time from B to A between t_1 and $t_1 + dt_1$, the quantity $j(t_2-t_1)dt_2$ is the fraction of trajectories that having arrived in well A at time t_1 cross for the first time back into B between t_2 and $t_2 + dt_2$, and the quantity $P(t-t_2)$ is the fraction of trajectories that have never left B by time t given that they

first entered B at time t_2 . It follows that $\int_0^t dt_2 \int_0^{t_2} dt_1 P(t-t_2)j(t_2-t_1)j(t_1)$ is simply the fraction of trajectories that have undergone the sequence of transitions $B \rightarrow A \rightarrow B$ in time t . The third term in Eq.(3.8) represents trajectories making the sequence of crossings $B \rightarrow A \rightarrow B \rightarrow A \rightarrow B$ in time t . In this way, it is easy to write the term corresponding to the sequence $B \rightarrow (A \rightarrow B)^n$. Eq.(3.8) represents the summation of all such terms for $n = 1$ to ∞ . Laplace transformation of Eq.(3.8) gives

$$\langle \tilde{\theta}(s) \rangle_+ = \tilde{P}(s) \sum_{n=0}^{\infty} [\tilde{j}(s)^2]^n \quad (3.9)$$

where $\tilde{P}(s)$ and $\tilde{j}(s)$ are the Laplace transforms of $P(t)$ and $j(t)$ respectively. Since $j(t) = -\partial_t P(t)$, $\tilde{P}(s) = (1 - \tilde{j}(s))/s$. Summation gives

$$\langle \tilde{\theta}(s) \rangle_+ = \frac{1(1 - \tilde{j}(s))}{s(1 - \tilde{j}(s)^2)} = \frac{1}{s} \frac{1}{1 + \tilde{j}(s)}. \quad (3.10)$$

To calculate $\langle \theta[x(t)] \rangle_-$ we must recognize that the trajectories start out moving towards well A. Thus we must consider the fraction of trajectories corresponding to $(A \rightarrow B)^n$ for $n = 1$ to ∞ . This gives

$$\begin{aligned} \langle \tilde{\theta}(s) \rangle_- &= \tilde{P}(s)\tilde{j}(s) \sum_{n=0}^{\infty} [\tilde{j}(s)^2]^n \\ &= \frac{1}{s} \frac{\tilde{j}(s)(1 - \tilde{j}(s))}{1 - \tilde{j}(s)^2} = \frac{1}{s} \frac{\tilde{j}(s)}{1 + \tilde{j}(s)}. \end{aligned} \quad (3.11)$$

From Eq.(3.5) it follows that the Laplace transform of the reactive flux is given by

$$\tilde{k}(s) = \langle \theta(s) \rangle_+ - \langle \theta(s) \rangle_- = \frac{1}{s} \frac{1 - \tilde{j}(s)}{1 + \tilde{j}(s)} \quad (3.12)$$

or

$$\tilde{k}(s) = \frac{\tilde{P}(s)}{2 - s\tilde{P}(s)} \quad (3.13)$$

which is our principal result.

The following model provides some insight. Assume that the fraction of particles entering the well at $t = 0$ which have not recrossed the transition state by time t is

$$P(t) = (1 - T_0)\theta(-t) + T_0e^{-k_2t}. \quad (3.14)$$

where $(1 - T_0)$ is the fraction of trajectories which quickly leave well B and $T_0e^{-k_2t}$ represents the trajectories which are trapped and subsequently leave with rate constant k_2 (or equivalent mean first passage time k_2^{-1}). The Laplace transform of $P(t)$ is

$$\tilde{P}(s) = \frac{T_0}{s + k_2}. \quad (3.15)$$

Inserting Eq.(3.15) in Eq.(3.13) and Laplace inverting gives

$$\hat{k}(t) = \frac{T_0}{2 - T_0} e^{-2k_2t/(2-T_0)}. \quad (3.16)$$

The prefactor is the plateau value for the rate constant and the transmission coefficient is

$$\kappa = \frac{k_f + k_b}{k_{TST}} = \frac{T_0}{2 - T_0}. \quad (3.17)$$

From Eq.(3.3) we recognize the argument of the exponential to be

$$k_f + k_b = \frac{2k_2}{2 - T_0}. \quad (3.18)$$

Combining Eqs.(3.17) and (3.18) we find

$$k_{TST} = \frac{2k_2}{T_0} \quad (3.19)$$

where the transition state rate constant is given simply in terms of the fraction of trajectories trapped quickly, T_0 , and the rate for once trapped trajectories to pass out of the well to the transition state, k_2 .

T_0 and k_2 can be found by taking a single well with an absorbing boundary at the transition state. The trajectories are sampled as in the calculation of $\hat{k}(t)$ (c.f. Eq.(3.5)); however, when a trajectory recrosses the transition state we remove it. After a short time all the trajectories that leave quickly are absorbed and the fraction of trapped trajectories decays as $T_0 e^{-k_2 t}$ so that k_2 may be found from this long time exponential decay. Eq.(3.13) may easily be extended to the case of the asymmetric double well potential. We find

$$\tilde{k}(s) = \frac{\tilde{P}_+(s)\tilde{P}_-(s)}{\tilde{P}_+(s) + \tilde{P}_-(s) - s\tilde{P}_+(s)\tilde{P}_-(s)} \quad (3.20)$$

where $\tilde{P}_+(s)$ and $\tilde{P}_-(s)$ are the Laplace transformed well populations for particles which have not recrossed the transition state from wells A and B, respectively. If we calculate the reactive flux for the asymmetric double well potential using Eq.(3.20) along with

$$\tilde{P}_\pm(s) = \frac{T_\pm}{s + k_\pm} \quad (3.21)$$

we find that

$$k(t) = \frac{T_+ T_-}{T_+ + T_- - T_+ T_-} \exp\left[-\frac{(T_+ k_+ + T_- k_-)t}{(T_+ + T_- - T_+ T_-)}\right]. \quad (3.22)$$

Combining Eqs.(3.3),(3.4), and (3.22), the transition state theory rate constant is found to be

$$k_{TST} = \frac{k_+}{T_+} + \frac{k_-}{T_-}. \quad (3.23)$$

3.3 Numerical Results

The reactive flux has proved useful in simulations of reactions in condensed matter. These studies involve the solution of the equations of motion of a large number of molecules and require considerable CPU time. Even when the solvent is represented as a stochastic bath the simulations require much more time especially when the friction coefficient is very large or very small. The absorbing boundary method leads to a considerable saving of computer time in these simulations.

To test the accuracy of the absorbing boundary method in determining the transmission coefficient, κ , we have simulated a one-dimensional system using Langevin dynamics. The potential is piecewise parabolic with barrier height Q , reactive well frequency ω_0 , and barrier frequency ω_B . The equation of motion is the Markovian Langevin equation, Eq.(2.3), where the Gaussian random force $R(t)$ has covariance $\langle R(0)R(t) \rangle = 2k_B T \gamma \theta(t - \tau_c) / \tau_c$ and τ_c is the correlation time of the force. These equations were integrated using an Adams-Moulton Predictor-Corrector algorithm [1] for $\beta Q = 10$, $\omega_B / \omega_0 = 2$, and 1000 trajectories for varying γ and τ_c . τ_c was adjusted to insure the system dynamics were Markovian. The initial state distribution was chosen according to the distribution $P^{(\pm)}(\mathbf{I})$ given by Eq. (3.6). In this

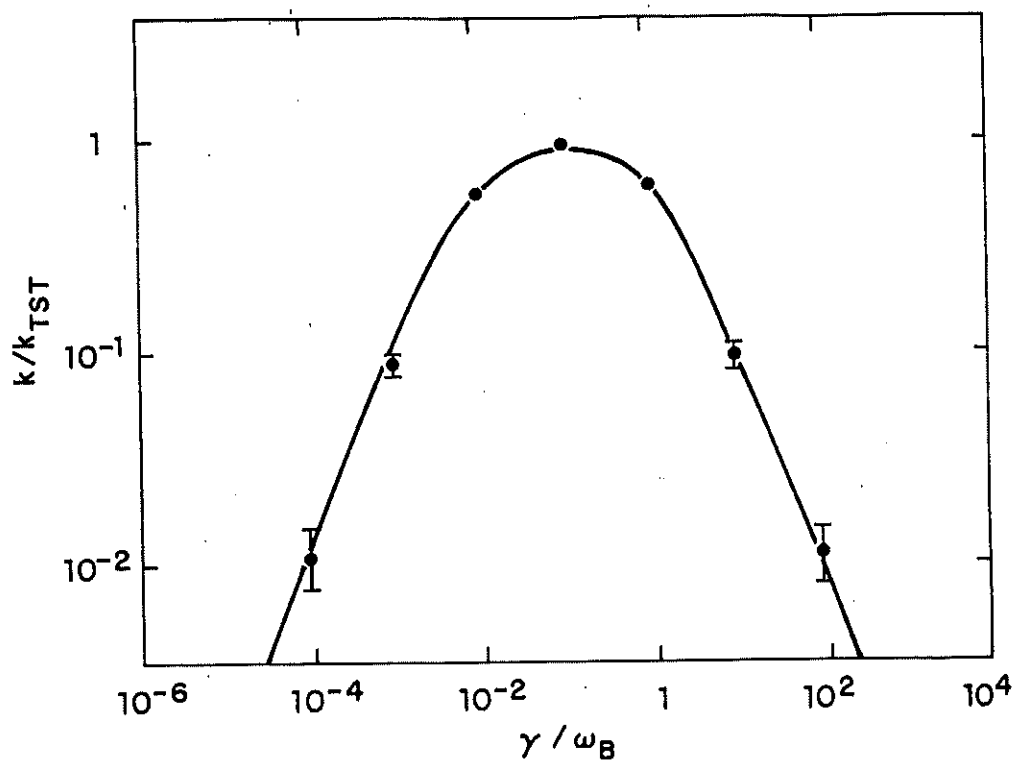


Figure 4: Numerical rate constants (\bullet) compared with Kramers' theory ($—$) for a one-dimensional Markovian system.

one-dimensional model, the position is initially constrained to the transition state while the velocity corresponds to the weighted distribution $ve^{-\beta v^2/2}$. The velocities were generated using the Box-Mueller sampling procedure (see Appendix).

The prediction of Kramers' theory (Chap. 2, Eqs.(2.5),(2.13), and (2.18)) for the overall rate constant k/k_{TST} is compared with the simulation results obtained using the absorbing boundary method in Fig. 4. Error bars give the 95% confidence interval. We find excellent agreement between theory and simulation in both the low and high γ limits (Fig. 4). The simulation

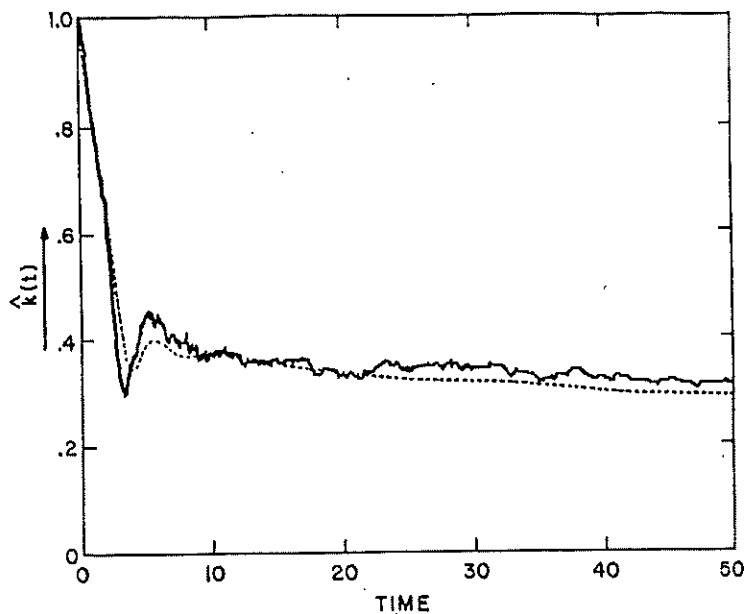


Figure 5: Reactive flux as predicted by Eq.(3.13).

data compare well with Kramers' theory in the asymptotic, low and high γ , regions. This lends support to the validity of the assumption underlying the absorbing boundary method. Further, the good agreement in the intermediate region supports the validity of the connection formula, Eq. (2.18).

As a further test of how well the absorbing boundary method reproduces the full reactive flux we have substituted the numerical Laplace transform of the simulated well population $P(t)$ into Eq.(3.13). This gives an approximation to $\tilde{k}(s)$. Inverse Laplace transformation of $\tilde{k}(s)$ gives the time dependent reactive flux $\hat{k}(t)$ defined by Eq. (3.2).

In Fig. 5 the exact normalized reactive flux, $\hat{k}(t)$, is plotted as a function of time (—) against the inverse Laplace transform of Eq.(3.13) (···) using the simulation results for the well population $P(t)$. The agreement is very good.

The absorbing boundary method even shows the wiggle in the transient decay regime. These tests indicate that the absorbing boundary method is accurate and useful for determining reaction rates and fluxes.

3.4 Discussion

We have shown how the rate constants $k_f + k_b$ and k_{TST} , and even the time dependence of the decay of $\hat{k}(t)$, may be found using the parameters for trapping and escape from a single well with an absorbing boundary at the transition state. The main assumption in our model is that the distribution of particles on recrossing the transition state is given by the distribution $P^{(\pm)}(\Gamma)$. This assumption is expressed by the simple product of fluxes in Eq.(3.8).

It is useful to test this assumption before applying the absorbing boundary method. We thus analyze the trajectories as they are absorbed for the first time. Fig. 6 displays the velocity distributions for particles recrossing the transition state as they are absorbed. The continuous line shows the exact velocity distribution given by $P^{(+)}(\Gamma)$, Eq.(3.6). The histogram displays normalized velocity distributions of those trajectories which recross quickly, numbering $1000(1 - T_0)$.

In the high friction regime, $\gamma/\omega_B = 10$, the velocity distribution agrees with $P^{(\pm)}(\Gamma)$ implying that the absorbing boundary method should be an excellent approximation for this case. In the low friction regime, for $\gamma/\omega_B = .01$, however, the agreement is less satisfactory. This can be understood as follows. At low γ the momentum relaxation time will be long compared

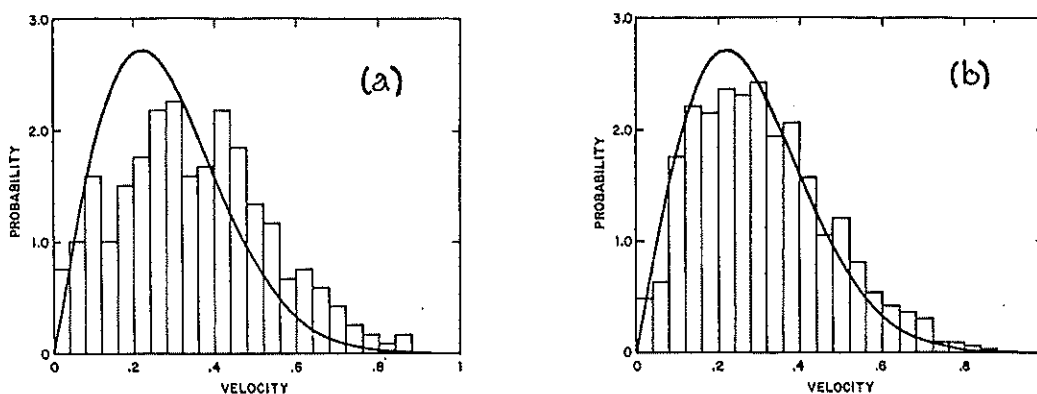


Figure 6: Velocity distributions for trajectories absorbed at the transition state for a) $\gamma/\omega_B = .01$ and b) $\gamma/\omega_B = 10$.

to the time spent in the well by those particles recrossing quickly. If the trapping probability decreases with the initial total energy, the low energy trajectories will be trapped more frequently than others. Since the relaxation time is long, the particles recrossing will not relax quickly enough to conform to $P^{(\pm)}(\Gamma)$ and so we find deviations. Although these deviations give some indication of the accuracy of the absorbing boundary method, even for low friction, $\gamma = .01$, the method produces a value of κ in agreement with the Kramers result.

It is useful to make an estimate of the time saved using the absorbing boundary method. Let τ_{rf} and τ_{ab} denote the integration time required to determine κ and $k_f + k_b$ using the reactive flux method and the absorbing boundary method, respectively. To determine τ_{rf} , N trajectories are followed for a time τ_λ necessary to determine $\kappa e^{-(k_f+k_b)t}$. Then $\tau_{rf} = N\tau_\lambda$. To determine τ_{ab} each of the N trajectories are followed until absorbed. Since

$P(t) \approx T_0 e^{-k_2 t}$ is the probability that a trajectory has not yet left well B in time t the average time that a trajectory is followed is

$$\langle \tau \rangle = \int_0^{\tau_\lambda} dt e^{-k_2 t} = \frac{1}{k_2} (1 - e^{-k_2 \tau_\lambda}). \quad (3.24)$$

Since $N(1 - T_0)$ trajectories are rapidly absorbed and NT_0 trajectories are followed on the average for time $\langle \tau \rangle$, it follows that $\tau_{ab} = NT_0 \langle \tau \rangle$ so that $\tau_{ab}/\tau_{rf} = T_0(1 - e^{-k_2 \tau_\lambda})/k_2 \tau_\lambda$. Since $T_0 \ll 1$ in either the very high or very low friction regimes, it follows then that $\tau_{ab}/\tau_{rf} \ll .1$ and the absorbing boundary method is preferred over the reactive flux method. For $k_2 \tau_\lambda > 1$ there is a further reduction in the time required for this method. It always pays to use this method. In the comparison with Kramers' theory the points in the very low ($\gamma = 10^{-4}$) and very high ($\gamma = 10^{-2}$) friction limits correspond to values of τ_{ab}/τ_{rf} equal to .021 and .022, respectively. In such cases a full determination of the reactive flux would take prohibitively long times.

4 One-dimensional Non-Markovian Systems

All realistic solvents have a finite relaxation time. This finite relaxation time is due to solvent memory effects in the form of high frequency collisions extending over finite periods of time, and low frequency, collective hydrodynamic effects[54]. It has been popular to model the system dynamics using the generalized Langevin equation[55,4,39], Eq.(2.6), where $\zeta(t)$ is the time dependent friction kernel. As discussed in Chap. 2, the best theoretical rate constant for a one-dimensional non-Markovian system as a function of friction is given by the connection formula of Hynes, Eq.(2.18), where the energy diffusion rate is given by Eq.(2.9), and the spatial diffusion rate constant is the Grote-Hynes rate, Eq.(2.13). In this section, simulation results will be presented which test the approximations intrinsic to Eq.(2.18).⁶

4.1 The Model

The system consists of a one-dimensional bistable piecewise parabolic potential with well and barrier frequencies ω_0 and ω_B , respectively. The friction is modeled as a single exponential

$$\zeta(t) = \frac{1}{\alpha} e^{-t/\alpha\gamma} \quad (4.1)$$

with correlation time $\tau_c = \alpha\gamma$ where α is a constant and γ is the zero frequency friction. Large α implies a strongly non-Markovian solvent with a

⁶Much of the material presented in this chapter appears in J.E.Straub, M.Borkovec and B.J.Berne, *J. Chem. Phys.*, 83:3172, (1985) and J.E.Straub, M.Borkovec and B.J.Berne, *ibid.*, 84:1788, (1986), Erratum and addendum, *ibid.*, 86:1079, (1987).

long relaxation time. The Markovian limit is reached as $\alpha \rightarrow 0$. The barrier energy is Q . The units are determined by taking the barrier frequency, ω_B , the particle mass, and the barrier energy Q to be unity.

All rate constants were calculated using the absorbing boundary method (Chap. 3). The equations of motion for the system follow from the fact that the one-dimensional generalized Langevin equation with exponential friction kernel can be expressed in terms of three Markovian equations[70,43]

$$\begin{aligned}\dot{x} &= v \\ \dot{v} &= -\frac{\partial U(x)}{\partial x} + z \\ \dot{z} &= -\frac{1}{\alpha}v - \frac{1}{\alpha\gamma}z + \xi\end{aligned}\tag{4.2}$$

where the fluctuation dissipation theorem for $\xi(t)$ is given by

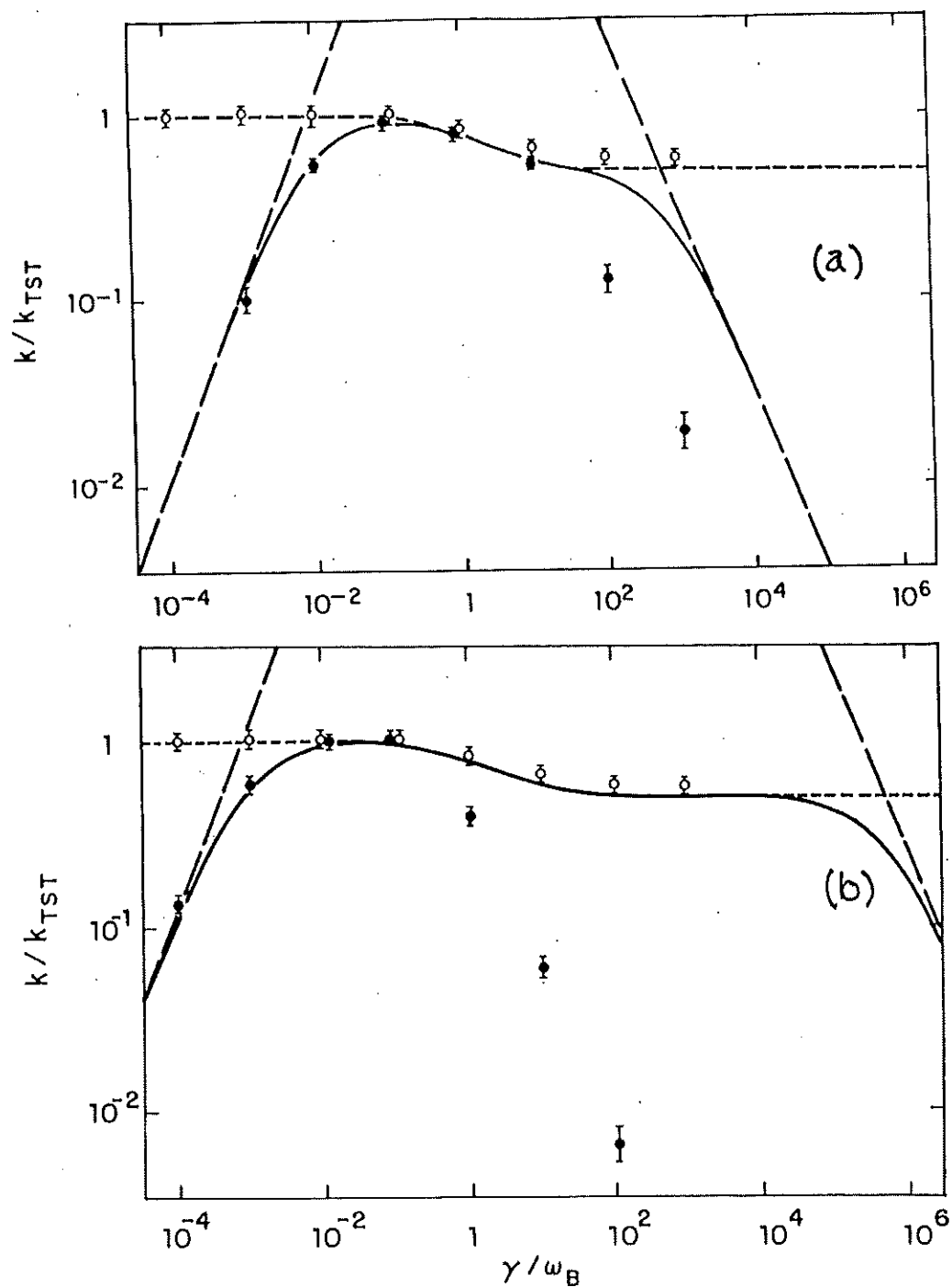
$$\langle \xi(t)\xi(0) \rangle = \frac{2}{\alpha^2\beta\gamma}\delta(t).\tag{4.3}$$

These equations were integrated using an Adams-Moulton predictor corrector algorithm[1]. The random force $\xi(t)$ was kept constant during each time step (Sec. 3.3). Initially, x , v , and z are sampled from the equilibrium distribution, Eq. (3.6), such that x is the position of the transition state surface at the barrier maximum, v is sampled from the equilibrium distribution $ve^{-\beta v^2/2}$, and z is sampled from $e^{-\alpha\beta z^2/2}$. The Box-Mueller sampling procedure was used (see Appendix). A typical calculation for a single rate constant involved 1000 trajectories and required from 10 minutes to several hours on an FPS-164 attached processor.

It is important to note the difficulty in obtaining rate constants at high γ . With increasing γ the correlation time of the friction increases and the initial transient terms in the calculation of the survival probability $P(t)$ (Chap. 3) will decay more and more slowly. Remember that one must integrate past the transient decay to insure that the plateau region is reached. As a rule of thumb, it is best to integrate the population until it is found to be constant over an order of magnitude in time. Since the relaxation time of the friction increases as γ (Eq.(4.1)), so will the endpoint of a given calculation. This does not, however, imply that the calculation using the absorbing boundary method will also increase as γ . While the CPU time required for a reactive flux calculation increases as the endpoint of the calculation (see Sec. 3.4), the CPU time required by the absorbing boundary method increases as the calculation endpoint times the fraction of surviving trajectories (Sec. 3.4). At large γ , the rate constant varies inversely with γ and therefore the actual calculation time required by the absorbing boundary method is approximately constant!

4.2 Numerical Results

The results are displayed in Fig. 7 where the transmission coefficient $\kappa = k/k_{TST}$ is plotted as a function of the static friction γ for $\beta Q = 20$ and $\alpha\omega_B^2 = 4/3$ for two different values of the frequency ratio a) $\omega_B/\omega_0 = 20$ and b) $\omega_B/\omega_0 = 2$. The simulation for the full potential (\bullet) and the inverted parabola (\circ), for which the theory of Grote and Hynes should be most accurate, are shown with error bars representing the 95% confidence

Figure 7: Rate constants as a function of γ .

interval. The theoretical predictions are displayed for the energy diffusion rate Eq.(2.9) (---), the Grote-Hynes rate Eq.(2.13) (- - -), and the connection formula Eq.(2.18) (—).

In both Figs. 7 a and b the simulation data for the full potential agree well with the predictions of the energy diffusion theory at small γ , increasing linearly with increasing γ . However, at large γ in both cases the rate constants are substantially overestimated by the theoretical predictions. At high γ , the measured rate decreases with increasing γ as $1/\gamma$.⁷

The theory of Grote and Hynes consists of approximating the rate constant for saddle crossing from reactant well to product well by the rate for crossing a harmonic barrier at the saddle point. The problem was approximately solved by expanding the potential in the barrier region as an inverted parabola with frequency ω_B and assuming a steady state distribution of states outside the barrier region[39,41]. Therefore, any contributions due to nonlinearities in the force or deviations from the steady state distribution at the barrier would not be described by the connection formula Eq.(2.18).

Figs. 7a and b also display simulation data for the inverted parabolic barrier in the absence of the reactant and product wells. The data is in good agreement with the Grote-Hynes rate constant for all γ . This indicates that the failure of the interpolation formula Eq.(2.18) to describe the rate for the

⁷A number of checks on the calculational procedure were performed. First, the small α limit was taken to insure that the calculated rates approached the Markovian Kramers' prediction. Second, the large α limit was taken where the rate limiting step is energy diffusion over the entire range of γ . Good agreement was found for small and large γ .

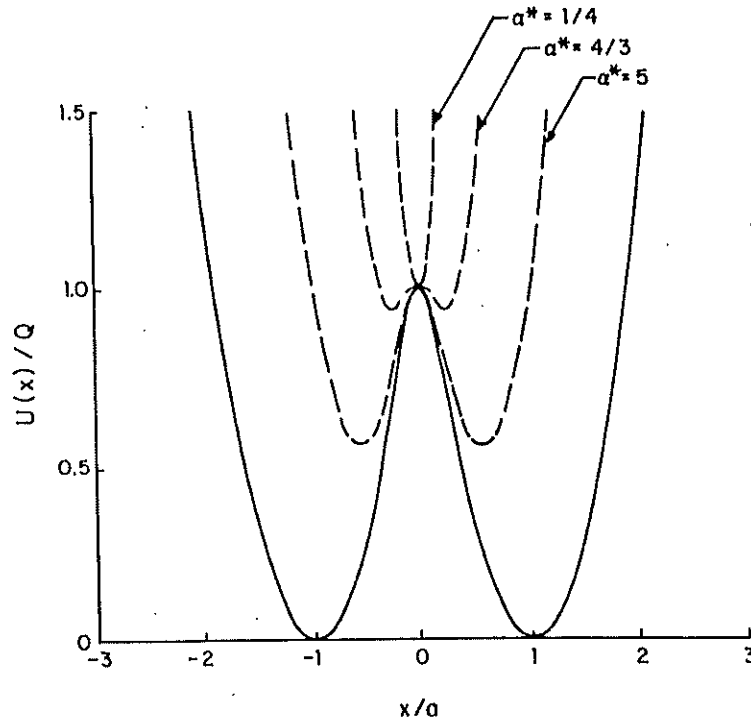


Figure 8: Effective potential of Eq.(4.4).

double well potential is due to dynamics involving the anharmonic regions of the potential.

To better appreciate the origin of these deviations, we examine the short time behavior of the equations of motion for trajectories starting at the transition state. For short times, the friction kernel can be approximated by the constant $\zeta(0) \approx 1/\alpha$. Inserting this into the generalized Langevin equation, Eq.(2.6), results in Hamilton's equations for a conservative system with the potential

$$U_{eff}(x) = U(x) + \frac{1}{2\alpha}x^2 \quad (4.4)$$

where $U(x)$ is the piecewise parabolic potential. This potential is plotted in Fig. 8 for several values of the dimensionless quantity $\alpha^* = \alpha\omega_B^2$. For small α^* , the trajectory is caged at short times in a harmonic potential[110] while for larger α^* the effective potential is a double well with barrier height dependent on α^* as well as time. At longer times the effective potential relaxes to the bare potential $U(x)$.

A typical trajectory for the system corresponding to Fig. 7 b is shown in Fig. 9. Clearly, at short times the trajectory recrosses the transition state many times after reaching the turning points of the effective potential. These recrossings are not included in the connection formula Eq.(2.18) as they are due to the anharmonic parts of the potential. Further, note that the trajectory becomes trapped in the dynamic wells for many oscillations before being activated again and performing inertial recrossings of the transition state. This behavior is characteristic of trajectories in the underdamped, energy diffusion regime (see Fig. 2). Eventually, the effective potential relaxes and the center of the trajectory's oscillation drifts into the true well and becomes trapped. This behavior is characteristic of trajectories in the overdamped, spatial diffusion regime (see Fig. 3).

4.3 Discussion

For non-Markovian systems, trajectories may be effectively "trapped" in a dynamic double well potential with an energy barrier much smaller than that of the bare potential $U(x)$ and with wells positioned much closer to the

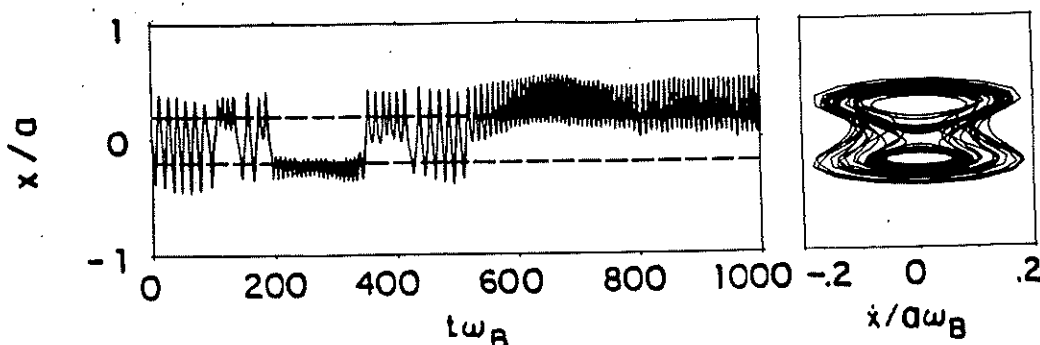


Figure 9: A trajectory showing short time structure of Eq.(4.4). $x = \pm a$ are the positions of the well minima while ω_B is the harmonic barrier frequency.

barrier maximum than are the wells of $U(x)$. This leads to short time multiple recrossings of the barrier not accounted for by either term in Eq.(2.18) resulting in much smaller rate constants.

Since energy diffusion is expected to be much faster in many dimensions (see Chap. 2), it might be expected that should a dynamic double well exist, rapid energy diffusion in many dimensions will cause trajectories to be trapped once they leave the barrier region thereby justifying the connection formula, Eq.(2.18). To understand this consider an N -dimensional potential consisting of a reactive coordinate coupled to $N - 1$ harmonic oscillators and experiencing diagonal exponential friction, i.e., there is no coupling between coordinates due to the friction tensor. The potential is simply

$$V(\mathbf{x}) = U(x_1) + \sum_{i=2}^N \left[\frac{\omega_i^2}{2} x_i^2 + \frac{\epsilon_i^2}{2\omega_i^2} x_1^2 + \epsilon_i x_i x_1 \right] \quad (4.5)$$

where $U(x_1)$ is the bistable piecewise harmonic potential of the reaction coordinate x_1 , ω_i is the harmonic frequency of the i th coupled oscillator, and

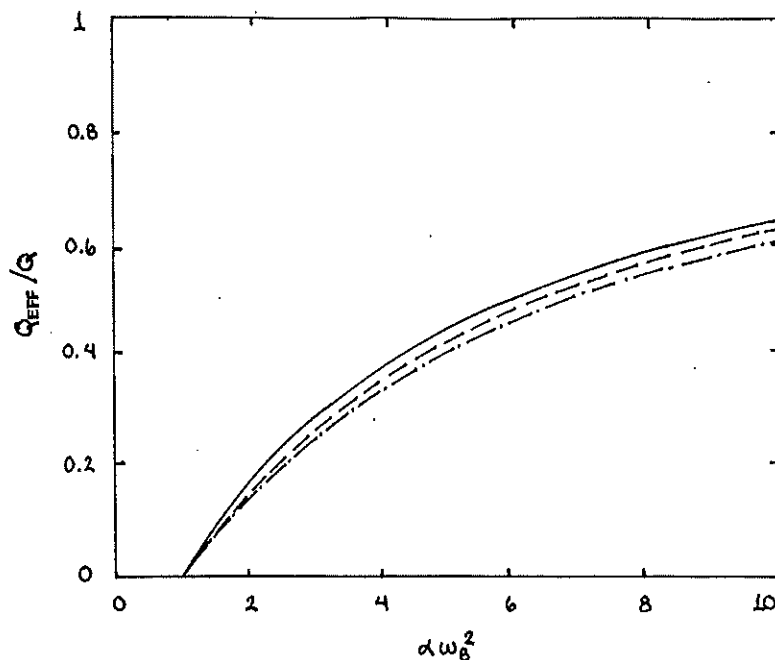


Figure 10: Barrier height of U_{eff} as a function of α .

ϵ_i is the constant coupling the i th oscillator to the reaction coordinate. The quadratic shift in x_1 insures that if one integrates over the $N-1$ coupled oscillators the potential projected on x_1 will be $U(x_1)$. For times short compared with the correlation time $\alpha\gamma$, the particle moves in the effective potential whose barrier height is shown in Fig. 10, with $\omega_B/\omega_0 = 2$, as a function of α for $N = 1$ (—), $N = 3$ (---), and $N = 5$ (- · -). For the assumptions of Eq.(2.18) to be met, where k_{GH} is the dominant contribution, a particle, after crossing the saddle and moving outside the barrier region, must relax in the well. This implies that the rate for energy diffusion in the well should be fast. For many dimensional systems, the energy diffusion rate constant is given by Eq.(2.11)[22], which varies approximately as the density of states of the reactant well. It depends strongly on the dimensionality of the system

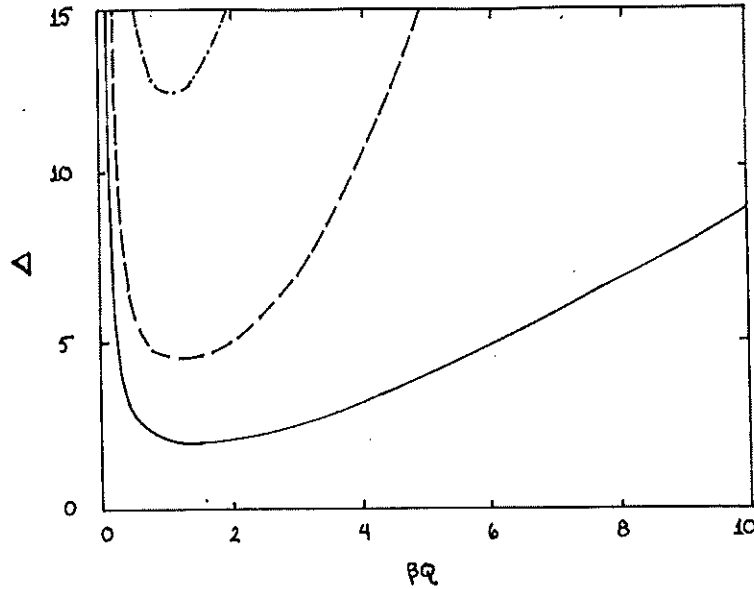


Figure 11: Prefactor for the energy diffusion rate Eq.(2.11).

as shown in Fig. 11 for $N = 1$ (—), $N = 3$ (- -), and $N = 5$ (- · -); $\Delta \equiv k_{ED} e^{\beta Q} / \sum_i \gamma_{ii}$ where k_{ED} is the energy diffusion rate for escape from a single well.⁸

We see in Fig. 10 that for the interesting case of $\alpha\omega_B^2 = 4/3$ the barrier height of the effective double well potential is rather small so that the energy diffusion rate is not strongly affected by an increase in the dimensionality and therefore the trapping probability is not significantly greater. This implies that for many dimensional systems, for certain values of α , we might expect the dynamic double well to cause recrossings and large deviations.

In addition to this effect, for many dimensional systems which are not strongly chaotic, as the friction is increased the number of modes participating in energy diffusion is reduced (Chap. 5). This would imply that

⁸I am grateful to Michal Borkovec for providing this figure.

while studies of isolated molecules indicate that many modes contribute to the rate, the dynamics of the solvated system may be described by substantially fewer coordinates. This would lead to fewer degrees of freedom in the effective potential, slower energy diffusion, and significant deviations from Eq.(2.18).

In conclusion, the above argument indicates that even for a molecule with many degrees of freedom, Eq.(2.18) may grossly overestimate the rate constant. The reactive degree of freedom experiences dynamic caging accompanied by very coherent recrossings of the barrier; a feature not anticipated by Eq.(2.18). Thus, a proper theory of reactions in a non-Markovian bath has not yet been devised.⁹

⁹Attempts at solving this problem have recently been published by Okuyama and Oxtoby[79,80]. They treat the position as the slow variable and try to calculate the first passage time for diffusion from the reactant to product well. We feel that this approach will not reproduce our data as Fig. 9 indicates that it is the energy, and not the position, that is the slow variable.

5 Two-dimensional Markovian Systems

In this chapter we examine the dynamics of barrier crossing using a two-dimensional Langevin equation in the low friction regime. We find that as the friction on the non-reactive mode is increased there is a transition from two-dimensional Markovian dynamics to one-dimensional non-Markovian dynamics resulting in a qualitative change in the behavior of the rate constant as a function of friction. This result supports the conclusion that existing theories which predict rates for energy activation in Markovian and non-Markovian systems have limited ranges of validity. A method is proposed which analyzes the eigenvalues of the full system and provides a criterion for the validity of the various theories. These ideas are then used to interpret the results of a recent experimental study. We also include a speculative discussion of the role of a random force in aiding intramolecular energy transfer.¹⁰

5.1 The Problem

The Langevin equations for N linearly coupled harmonic oscillators may be exactly reduced to a one-dimensional generalized Langevin equation whose time dependent friction kernel will depend on the frequency, friction, and coupling parameters of the eliminated coordinates. Similarly, the generalized Langevin equation, Eq.(2.6), may be transformed into a system of linearly coupled Markovian equations[75,16,104,45]. The number of resulting equations will in general depend on the time dependent friction kernel

¹⁰Much of the material presented in this chapter appears in J.E.Straub and B.J.Berne, *J. Chem. Phys.*, 85:2999, (1986).

used. A Gaussian kernel results in an infinite set of equations. An exponential kernel requires three equations and is not isomorphic with a Markovian Langevin equation. However, certain kernels do lead to an equivalence between Eqs.(2.6) and (2.10).

It is obvious that whether one chooses to model the reaction system with N coupled Langevin equations or the equivalent one-dimensional generalized Langevin equation, the results must be identical. However, the energy activation rate constants corresponding to these two models, given by Eqs.(2.11) and (2.9) respectively, are certainly *not* the same. They most obviously differ in their prefactors, which show a different dependence on βQ , and their frictional dependence, where Eq.(2.11) is a monotonically increasing function of the friction while Eq.(2.9) is capable of more complicated behavior. This implies that while the transformation from N linearly coupled Langevin equations to a one-dimensional generalized Langevin equation is exact, application of the corresponding theories for energy diffusion rates must be restricted.

The derivation of Eq.(2.8) for the rate of energy activation has as its basic equation of motion the Zwanzig equation for energy diffusion[119,24]. In the derivation of this equation, one assumption is that all those coordinates not treated explicitly, corresponding to those coordinates eliminated from the N -dimensional Langevin equation, must relax much faster than those coordinates treated explicitly.¹¹ At any point in time the eliminated

¹¹This is the first assumption of Ref. [119].

coordinates must be distributed according to their equilibrium thermal averages. The Zwanzig equation, and therefore Eq.(2.8), will be valid only when those coordinates which were eliminated from the corresponding set of coupled Langevin equations are overdamped.¹² We define N_{ISO} to be the total number of coordinates which are actively coupled to the internal potential in the isolated molecule. When all coordinates are underdamped and the full phase space is chaotic, Eq.(2.11) will accurately predict the rate of energy activation where $N = N_{ISO}$. As the damping on N_E of the N_{ISO} coordinates increases, to the point where they may be eliminated, the result is an effective $N_{EFF} = N_{ISO} - N_E$ dimensional generalized Langevin equation where the rate for energy activation will be given by the appropriate non-Markovian theory[117].

When the phase space is not fully chaotic, the prefactor in Eq.(2.11) will be reduced by the portion of regular phase space which does not contribute reactive trajectories[23]. In the limit where the friction goes to zero the random force fluctuations are very small and the rate reduces to Eq.(2.11) multiplied by X^\neq which is the measure in phase space of reactive trajectories[23,14]. For larger frictions and temperatures the random force fluctuations are larger and may lead to an increase in X^\neq .¹³

This is discussed further in Sec. 5.6.

¹²This condition has been clearly stated[119,24]; however, it was not closely followed in subsequent applications[25].

¹³The study of Berne [14], along with [23], examine only strong collision models. To say that the low friction limit of the weak collision model is given simply by Eq.(2.11) multiplied by X^\neq *assumes* that the energy diffusion coefficient $D(E)$ is the same as for the fully chaotic system.

5.2 A Model System

To make these ideas more concrete we examine the two-dimensional system

$$\begin{aligned}\ddot{x}_1 &= -\frac{\partial U(x_1)}{\partial x_1} - \epsilon x_2 - \gamma_1 \dot{x}_1 + R_1(t) \\ \ddot{x}_2 &= -\omega_2^2 x_2 - \epsilon x_1 - \gamma_2 \dot{x}_2 + R_2(t).\end{aligned}\quad (5.1)$$

A similar set of equations has been studied for weak coupling in both the underdamped and overdamped limits by Carmeli and Nitzan[25]. They transformed Eq.(5.1) into the corresponding generalized Langevin equation by elimination of x_2 and obtained

$$\ddot{x}_1 = -\frac{\partial U_{EFF}(x_1)}{\partial x_1} - \int_0^t dt' \zeta(t-t') \dot{x}_1(t') + R(t) \quad (5.2)$$

where the Laplace transform of $\zeta(t)$ is

$$\hat{\zeta}(s) = \gamma_1 + \frac{\epsilon^2}{\omega_2^2} \frac{s + \gamma_2}{s^2 + s\gamma_2 + \omega_2^2}. \quad (5.3)$$

and the effective potential is

$$U_{EFF}(x_1) = U(x_1) - \frac{\epsilon^2}{2\omega_2^2} x_1^2. \quad (5.4)$$

They concluded that when the non-reactive mode, x_2 , relaxed very quickly the time dependent friction kernel of Eq.(5.3) could be replaced by its zero frequency value resulting in a one-dimensional Markovian Langevin equation whose rate for energy activation would be given by Eq.(2.5) where

$$\gamma = \gamma_1 + \frac{\epsilon^2}{\omega_2^4} \gamma_2. \quad (5.5)$$

For the case where x_2 does not relax quickly, the one-dimensional non-Markovian result similar to Eq.(2.9) was applied over a large range of coupling where they found that the dependence of the rate constant on the activation energy, or temperature, was *not* affected by the mode-mode coupling.

In contrast to these results, our discussion implies that only for the case when the non-reactive mode relaxes quickly may Eq.(2.8), corresponding to the one-dimensional generalized Langevin equation, be used. When the non-reactive mode is underdamped we must use the two-dimensional result of Eq.(2.11) which, as we have mentioned, has a different temperature dependence than does Eq.(2.8).

5.3 Simulation Results

The transition state theory normalized rate constants were calculated using the rapid absorbing boundary version of the reactive flux (see Chap. 3). The runs were performed on an FPS-264 attached processor. The equations of motion were solved using an Adams-Moulton predictor-corrector algorithm[1]. The random force was taken to be a constant during each integration step[108]. An average calculation using 1000 trajectories required several hours of CPU time. To define the total rate constant, k , for all friction we use the connection formula Eq.(2.18) where k_{ED} is the appropriate energy diffusion rate theory.

We wish to examine this system when the the rate for energy transfer to the reaction coordinate is relatively slow. To do this we set $\gamma_1 = 0$ in

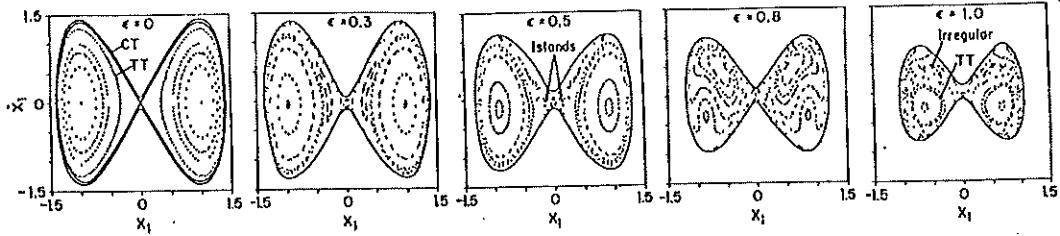


Figure 12: Poincaré surfaces of section.

Eq.(5.1) so that the bath acts directly only on the non-reactive coordinate x_2 and the equations of motion are

$$\begin{aligned}\ddot{x}_1 &= -\frac{\partial U(x_1)}{\partial x_1} - \epsilon x_2, \\ \ddot{x}_2 &= -\omega_2^2 x_2 - \epsilon x_1 - \gamma_2 \dot{x}_2 + R_2(t).\end{aligned}\quad (5.6)$$

We first examine the dynamics for the quartic reactive coordinate potential

$$U(x_1) = x_1^4 - \left(2 - \frac{\epsilon^2}{2\omega_2^2}\right)x_1^2. \quad (5.7)$$

To determine N_{ISO} , we characterized the corresponding Hamiltonian system by examining Poincaré surfaces of section for various values of the coupling strength ϵ (Fig. 12). These diagrams describe the qualitative behavior of the transition to chaos for the bistable potential of Eq.(5.7) for the reactive coordinate x_1 . The surfaces of section are shown for total energy $E = 1.01$ and coupling strength (indicated for each figure) which increases from left (no coupling) to right. For no coupling the phase space is fully regular with trapping tori, TT, and crossing tori, CT[31]. As the coupling is increased there is the destruction of TT and the formation of primary islands. At the

strongest coupling there is a large measure of phase space which is irregular while TT still exist.

We found that there is no strong, or first order, transition to chaos in this system. However, there is a sizable portion of phase space which is irregular for $\epsilon \geq .85$, while those portions which are regular often contain resonance tori which contribute to sizable resonant energy exchange between x_1 and x_2 . This is supported by the results of critical point analysis[27] which indicate that the global inversion symmetry of the potential is important in stabilizing the diverging trajectories in the saddle region. It is possible that in the presence of collisions the condition that the Hamiltonian system be chaotic for there to be equipartitioning in the dissipative system is too strong. Collisions coupled with resonant energy exchange may be sufficient to partition energy between modes effectively. This idea will be discussed in greater detail in Sec. 5.6.

We compare the simulation results with the theoretical predictions in Fig. 13 for the case of large ϵ leading to intermediate coupling. Rate constants are shown for the potential of Eq.(5.7) as a function of the static friction $\gamma = \gamma_2$ for $\beta Q = 5$, $\omega_2 = 0.75$, $\gamma_1 = 0$ and $\epsilon = 1.0$. The simulation data with error bars are represented by circles, (o). The theoretical predictions are represented by lines: Grote-Hynes theory for saddle crossing Eq.(2.13) (- · -), and the overall rate using the connection formula of Eq.(2.18) for one (— —) and two (—) dimensions, using k_{ED} from Eqs.(2.8) and (2.11), respectively.

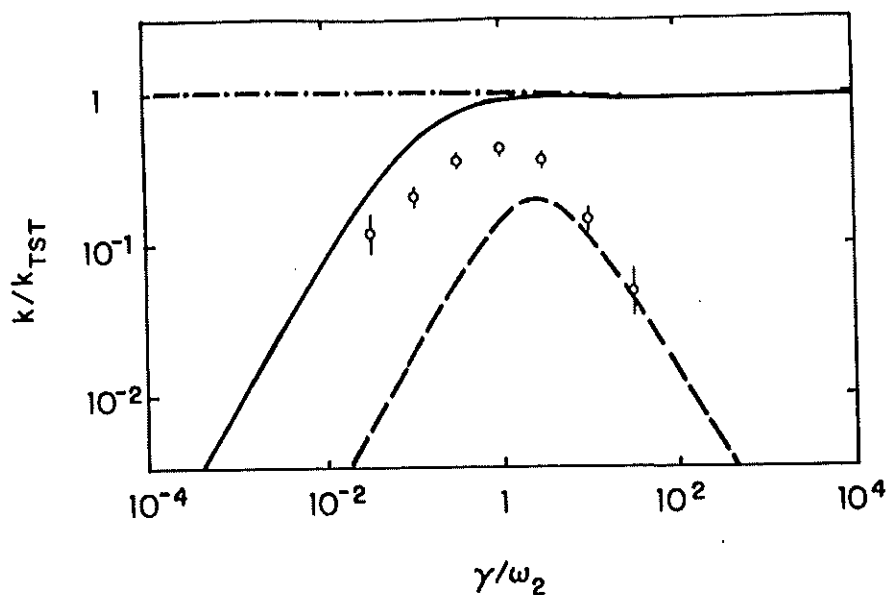


Figure 13: Rate constants for anisotropic friction.

For large γ the rate is accurately predicted by the one-dimensional theory.¹⁴ This is the adiabatic limit. As γ is decreased there is a gradual approach towards the two-dimensional Markovian theory. This is expected, as for smaller γ the rate for energy transfer between x_1 and x_2 becomes comparable to the rate for energy activation and so a larger portion of phase space contributes reactive trajectories leading to an increased initial slope of the rate constant as a function of γ .

For the case of isotropic friction, corresponding to Eq.(5.1) with $\gamma_1 = \gamma_2$, the reaction coordinate x_1 directly experiences a friction and random force. In Fig. 14 the simulation results are compared with theoretical predictions. Rate constants for the potential of Eq.(5.7) as a function of the static friction $\gamma = \gamma_2$ are shown with $\beta Q = 5$, $\omega_2 = 0.75$, $\gamma_1 = \gamma_2$ for a) $\epsilon = 0.3$ and b)

¹⁴The rate was calculated using Eq.(2.8) with Eqs. (2.7) and (2.8a) of Ref. [118]

$\epsilon = 1.0$. The simulation data with error bars are represented by circles. The theoretical predictions are represented by lines as described for Fig. 13.

The predicted rate for one-dimensional energy diffusion is much faster than the anisotropic case above. For very large γ , the rate is limited by spatial diffusion across the saddle. For small ϵ and weak coupling, Fig. 14a shows the rate constants are accurately predicted by the one-dimensional theory over the full range of γ simulated. For large ϵ and intermediate coupling, Fig. 14b shows that at large γ the rate is accurately predicted by the saddle crossing theory while for smaller friction the simulation results approach the two-dimensional theory.

5.4 Adiabatic Elimination

We would like to be able to predict when the transition from two to one-dimensional dynamics is complete as the friction is increased, i.e., that value of the friction above which the rate constant is predicted by the one-dimensional theory. We concentrate on the case where $\gamma_1 = 0$ (Fig. 13). We define a transition value of γ_2 as the *approximate* value of γ_2 separating the two and one-dimensional dynamics. The theory of “slaving,” or adiabatic elimination of variables[42], predicts that when γ_2 is large, so that x_2 is overdamped, one may set $\ddot{x}_2 = 0$ in Eq.(5.6) and disregard the random force. We may then integrate in time to get x_1 in terms of x_2 and substitute in Eq.(5.6) to find an equation similar to Eq.(5.2) with

$$\hat{\zeta}_{AE}(s) = \frac{\epsilon^2}{\omega_2^2} \frac{\gamma_2}{s\gamma_2 + \omega_2^2}. \quad (5.8)$$

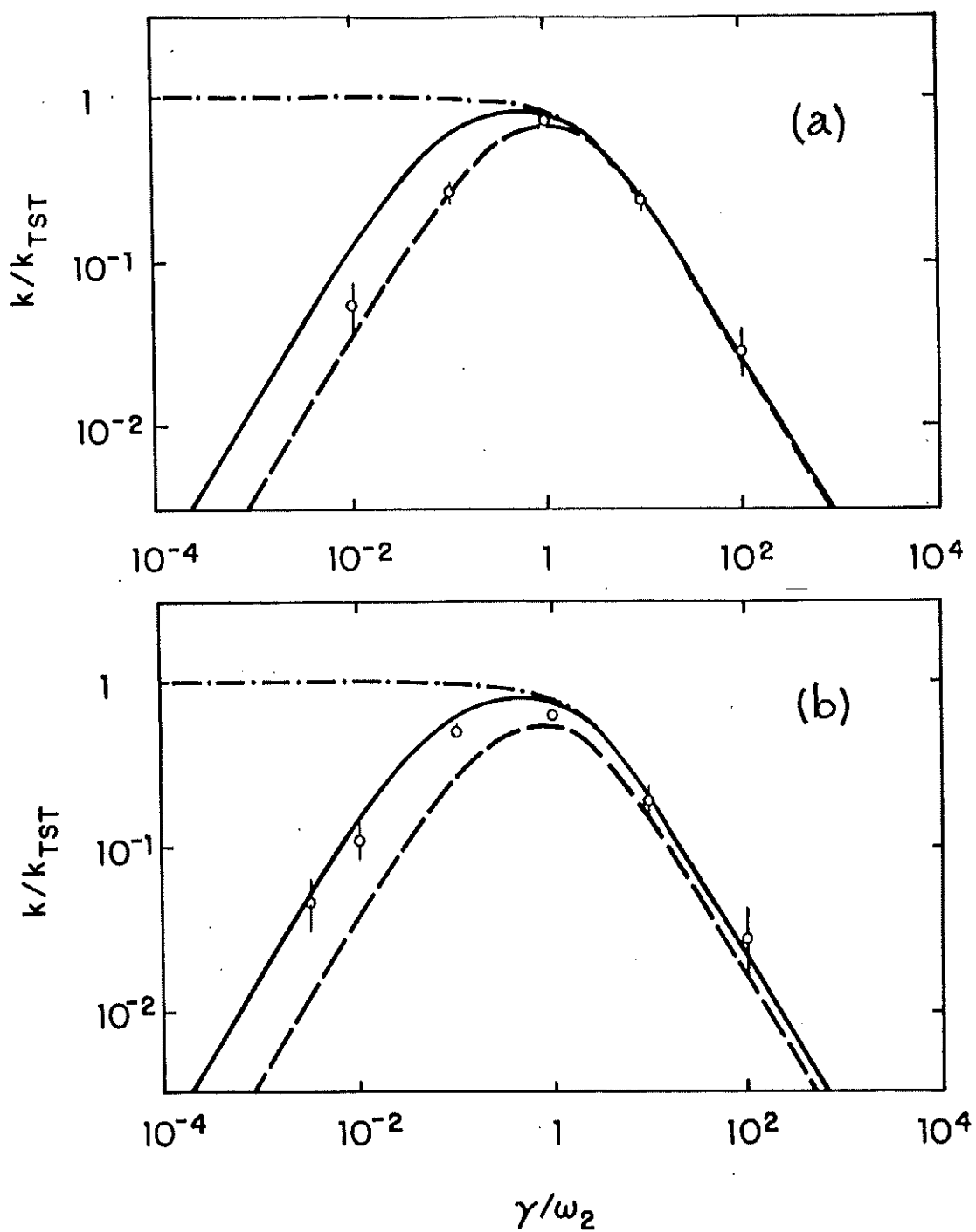


Figure 14: Rate constants for isotropic friction.

If we use Eq.(5.8) in Eq.(2.8) we find, as expected, that for small γ_2 the result differs dramatically from the result using the exact friction kernel of Eq.(5.3). However, as γ_2 is increased, after some $\gamma_2 \gg \omega_2$ the adiabatic result agrees well with the exact result. *The transition value from adiabatic elimination, γ_{AE} , would be roughly that γ_2 where the adiabatic result is approximately equal to the result from full elimination.*

Comparison with Fig. 13 shows that the transition occurs at $\gamma_2 < \gamma_{AE}$ so that this criterion is too strong. We therefore need a criterion which is more sensitive to the internal dynamics of the system.

5.5 Eigenvalue Analysis

Another possibility lies in analyzing the behavior of the system eigenvalues as a function of the friction.¹⁵ Since we are interested in energy diffusion, and therefore the dynamics in the wells, we first linearize Eq.(5.6) about the well minima and then Laplace transform, disregarding initial condition terms and fluctuating forces, we find the equation for the Laplace variable s

$$s^4 + s^3(\gamma_1 + \gamma_2) + s^2(\omega_1^2 + \omega_2^2 + \gamma_1\gamma_2) + s(\gamma_1\omega_2^2 + \gamma_2\omega_1^2) + \omega_1^2\omega_2^2 - \epsilon^2 = 0 \quad (5.9)$$

where ω_1 is the frequency of the harmonic approximation to the reactive coordinate well frequency. The roots of this equation are the system eigenvalues. That Eq.(5.9) is a fourth degree polynomial indicates that there are four roots corresponding to the four degrees of freedom in the system, x_1 , x_2 , \dot{x}_1 and \dot{x}_2 .

¹⁵This idea is central to the qualitative theory of differential equations[8]. Similar ideas have been used by Hänggi to examine the validity of the Grote-Hynes relation[44].

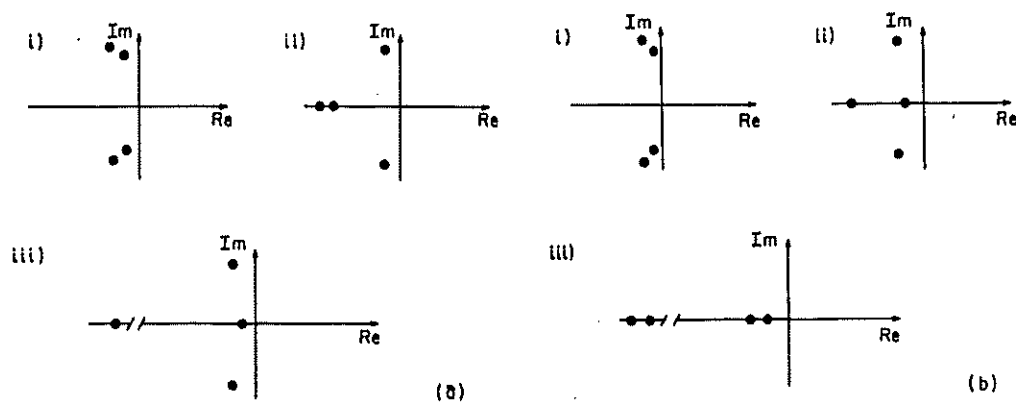


Figure 15: Schematic diagram of eigenvalues in various friction regimes.

Fig. 15 describes the qualitative behavior of the eigenvalues for a) the anisotropic system of Fig. 13 where $\gamma = \gamma_2$ and $\gamma_1 = 0$ and b) the isotropic system of Fig. 14b where $\gamma = \gamma_2$ and $\gamma_1 = \gamma_2$, for various values of the static friction (i) $\gamma < \gamma_{BI}$, (ii) $\gamma \approx \gamma_{BI}$, and (iii) $\gamma > \gamma_{BI}$. γ_{BI} is the approximate transition value, derived from the eigenvalue analysis, above which the rate constant should agree with the one-dimensional theory. In Fig. 15a, for small γ the roots consist of two complex conjugate pairs whose imaginary parts are much greater than their real parts. This implies that the system motion is highly oscillatory or underdamped. As γ is increased to γ_{BI} , one complex conjugate pair moves onto the real line and bifurcates. One of the resulting real eigenvalues increases in magnitude with increasing γ while the other decreases becoming small negative. The other complex conjugate pair remains complex for all γ indicating that the corresponding modes are always underdamped.

This is clearly seen in Fig. 16. The ratio of the imaginary to real parts of the system eigenvalues is plotted as a function of γ for a) the anisotropic system of Fig. 13 and b) the isotropic system of Fig. 14b. The various approximations for the transition value for γ are marked on the abscissa. As γ is increased we find that for one complex conjugate pair the real part approaches in magnitude the imaginary part and then the imaginary part goes to zero at γ_{BI} , while the other pair decreases initially and then increases for $\gamma > \gamma_{AE}$.

We may then interpret the behavior in Fig. 13 of the anisotropic system, where $\gamma = \gamma_2$ and $\gamma_1 = 0$, as follows. For $\gamma \ll \gamma_{BI}$ the eigenvalues consist of two complex conjugate pairs indicating two-dimensional underdamped motion. Here we expect that for a strongly chaotic system, two-dimensional dynamics will apply and the rate will be best predicted by Eq.(2.11) multiplied by the proper factor, X^\neq , for the fraction of phase space contributing reactive trajectories[23]. For $\gamma > \gamma_{BI}$ the eigenvalues consist of one complex conjugate pair and one real pair. For couplings such that the major contribution to the reactive coordinate comes from the complex conjugate pair, the dynamics will correspond to one-dimensional energy diffusion of Eq.(2.8). For $\gamma \gg \gamma_{BI}$ we reach the adiabatic limit where Eq.(5.8) will apply. While the transition is not sharp, we expect the transition between one and two-dimensional energy diffusion to occur near γ_{BI} . Examining Fig. 16a we find that γ_{BI} most accurately predicts the value of the friction above which the system is one-dimensional, giving the least upper bound.

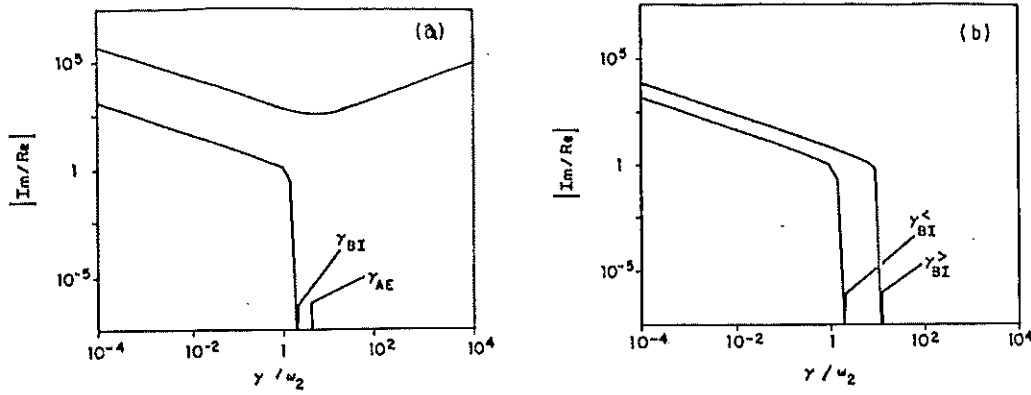


Figure 16: Eigenvalues as roots of Eq.(5.9) .

As another example of the eigenvalue method, we examine the dynamics of Eq.(5.1) for the case of isotropic friction, $\gamma = \gamma_1 = \gamma_2$. The qualitative behavior is shown in Fig. 15b. We find that at small γ the system eigenvalues consist of two complex conjugate pairs, whose imaginary parts greatly exceed their real counterparts. This indicates that the dynamics will correspond to two-dimensional energy diffusion. As γ is increased, one pair moves onto the real line at $\gamma_{BI}^<$ leaving one complex conjugate pair practicing one-dimensional energy diffusion. For $\gamma > \gamma_{BI}^>$ the system is characterized by two small and two large negative eigenvalues. This is the mark of a truly overdamped system, and spatial diffusion at the saddle will be rate limiting[44]. This reduced dimensionality leads to a reduction of the slope of the rate constant as the friction is increased. Therefore, as γ is increased we should first see two-dimensional energy diffusion followed by one-dimensional energy diffusion and a final transition to fully overdamped behavior where crossing

of the saddle is rate limiting. The simulation data shown in Fig. 14 support this conclusion.

In summary, for an N -dimensional Markovian system we may linearize the equations of motion in the well resulting in $2N$ eigenvalues which characterize the system dynamics. For small damping, the eigenvalues consist of N complex conjugate pairs with imaginary parts which greatly exceed their real counterparts. Here the dynamics should be described by N -dimensional energy diffusion. As the damping is increased, some N_E complex conjugate pairs move towards the real line. *When their imaginary parts approach in magnitude their real counterparts the motion will become overdamped in character and the corresponding coordinates may then be eliminated from the reaction system.* Here the dynamics will be described by N_{EFF} -dimensional energy diffusion. As long as the reaction coordinate itself is not overdamped the system dynamics will remain underdamped in character with successively fewer degrees of freedom contributing to the rate as the damping on the non-reactive modes is increased.

5.6 External Noise and Energy Transfer

For the purposes of this discussion we will confine ourselves to a bistable coordinate coupled to $N - 1$ oscillators. When the coordinates are uncoupled, the system is fully regular and there exist N constants of the motion for the system corresponding to the energies in each of the N independent coordinates. The phase space may be decomposed into KAM surfaces labeled crossing tori, CT, and trapping tori, TT [31,18]. In two dimensions the CT

form a separatrix which confines the TT to either the reactant or product region (Fig. 12). As the coupling is increased, the KAM surfaces forming the separatrix will begin to break down leading to the formation of islands and increasing areas of irregular phase space. At higher coupling, the TT will become unstable.

In highly nonlinear systems, for certain couplings and energy there may be a global transition to chaos where the full phase space is irregular. For other systems, such as Eqs.(5.6) and (5.7), there may be only a weak transition, i.e., for any value of the coupling there will still be preserved tori. In two dimensions, a KAM surface will form an uncrossable barrier. In three or more dimensions, all irregular regions of phase space are connected by an Arnold web and diffusion inside this web[65]. Other "partial barriers" exist. These may be Cantori[66,12] or KAM tori which are partially destroyed known as "vague tori"[88]. In each case, there is motion along these tori as well as slow diffusion across them.

For weak collision models, the random force produces jumps in the momentum which cause transitions both *along* and *between* surfaces of constant energy. An activated trajectory may be thought to move in an energy shell whose width is determined by the short time fluctuations in energy which leave the trajectory activated. Below we discuss several mechanisms acting in weak collision models which may lead to faster diffusion in the irregular portions of phase space, as well as an increased area of phase space contributing reactive trajectories. Fig. 17 is a schematic diagram describing

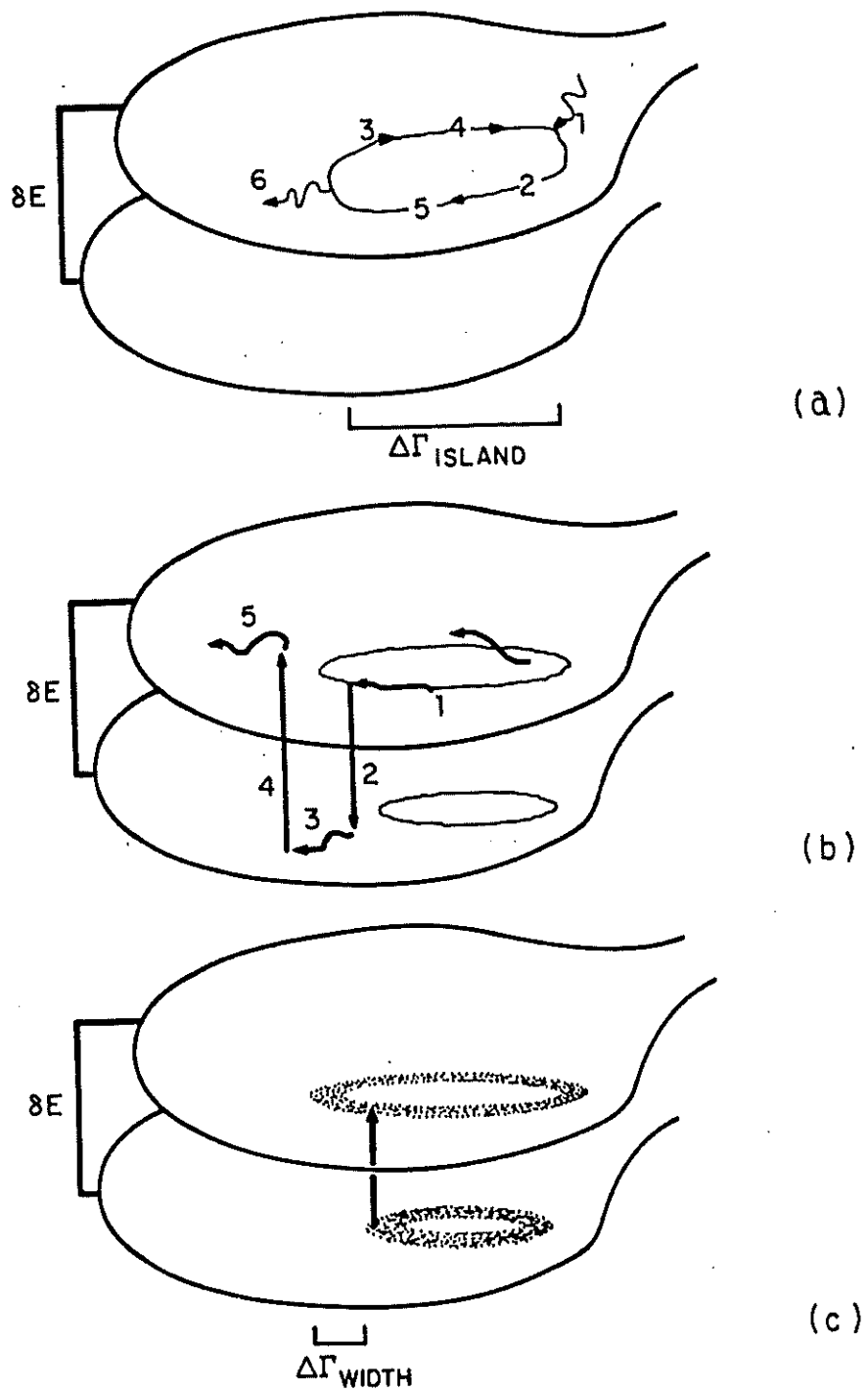


Figure 17: Schematic diagrams describing scenarios for the possible effect of external noise on trajectories in the energy diffusion regime.

the transition between adjacent energy levels due to perturbations from the random force.¹⁶ The various scenarios are described below.

5.6.1 Resonance Streaming

If the phase space is partially regular, containing large islands or KAM surfaces, a random force may lead to an increased rate of diffusion through the chaotic region[65]. An irregular trajectory moving near a KAM torus, in the form of an island, may be kicked onto the torus from an irregular region by the random force. The trajectory may then “stream” along the resonance surface for some time, its phase being randomized, before being kicked off into an irregular region (Fig. 17a). The solid line depicts the motion of a trajectory where the various fragments are labeled in the order of their occurrence.

If the torus is large, this may lead to a large jump in phase space and greatly enhanced diffusion. If the width of the island is $\Delta\Gamma_{island}$, and the time between transitions is τ , the diffusion due to resonance streaming will be approximately[65]

$$D_{RS} \approx \frac{\langle \Delta\Gamma_{island}^2 \rangle}{2\tau}. \quad (5.10)$$

5.6.2 Surface Crossing

A kick of the random force may simply move a trajectory off a KAM surface, if the perturbation is large enough that the motion becomes unstable. This

¹⁶I thank Anders Wallqvist for helping in the production of this figure.

will depend on the size of the stable region about the KAM surface and the size of the random fluctuations, which in turn depends on the temperature and friction.

A more complicated scenario for moving across a KAM surface is shown schematically in Fig. 17b where the solid line depicts the motion of two trajectories and the various fragments are labeled in the order of their occurrence. The position of the KAM surface in phase space may change for changing energy. In the case of motion in a well, the area of phase space for each energy level will increase with increasing energy. Therefore, a trajectory moving *on* or *in* a KAM surface may be kicked to a lower energy surface *off* or *outside* of the corresponding KAM surface. There it may diffuse in the surrounding region before undergoing a transition up in energy. After this transition, the trajectory may be outside the original KAM surface. This mechanism may act to accelerate diffusion across Cantori[66,12] as well as allow transitions across a KAM torus which would be forbidden in conservative systems.

5.6.3 Resonance Diffusion

This is similar to resonance streaming where the trajectory diffuses *within* a resonance width[65]. A trajectory diffusing in a well undergoes transitions in energy where the torus at higher energy is slightly displaced from the

torus at lower energy. This is depicted in Fig. 17c where the arrow indicates a transition between two resonances on adjacent energy levels. The surrounding shaded region indicates the width of each resonance.

If the difference in the torus position or size between energy levels is $\Delta\Gamma_{width}$, and the transition time is τ , the rate for diffusion is [65]

$$D_{RD} \approx \frac{\langle \Delta\Gamma_{width}^2 \rangle}{2\tau}. \quad (5.11)$$

In practice, some or all of these mechanisms may act to accelerate diffusion. The role that each plays will depend on the particular potential, the degree of irregularity, the detailed island structure, the temperature, and the friction.

5.7 Discussion

We have examined the dynamics of many dimensional Markovian systems, both strongly anisotropic and isotropic, over a wide range of friction. We find that the system dynamics depends on the damping felt by each coordinate and that examination of the system eigenvalues is important in understanding the behavior as a function of the friction coefficient. In particular, we have compared the predictions of current theories for energy diffusion with simulation results for a two-dimensional Markovian system in the weak and intermediate coupling regimes. We find that one-dimensional theories, which eliminate non-reactive coordinates and treat the reactive coordinate with a renormalized friction and potential, have a limited range of validity.

For small enough friction, the rate for energy transfer between the N_{ISO} coupled coordinates, assuming there is energy transfer, is faster than the rate

for energy activation. Therefore, all modes must be considered explicitly. The rate will be most accurately predicted by the N_{ISO} -dimensional Markovian theory of Eq.(2.11) with the proper prefactor for the measure of phase space contributing reactive trajectories. As the friction is increased on the non-reactive modes, these modes will eventually become overdamped so that their rate for energy transfer to the reactive mode is much less than the rate for energy activation. These modes, numbering N_E , may then be eliminated. The reaction system will consist of $N_{EFF} = N_{ISO} - N_E$ dimensions where the rate is in general predicted by the N_{EFF} -dimensional non-Markovian theory. Of course, depending on the friction kernels, it may be appropriate to use an N_{EFF} -dimensional Markovian theory[22]. This results in a rate for energy diffusion which is, for reasonably high barriers $Q \gg k_B T$, much less than that predicted by Eq.(2.11) using $N_{EFF} = N_{ISO}$. The approximate value of the friction for which elimination is valid may be determined by considering the quantitative features of the system eigenvalues.

In applying these ideas, one must consider the details of the various assumptions made. In the process of energy diffusion, a particle will gain energy through small jumps imparted by the random force. For very low friction, the trajectory will remain activated for a long time before being deactivated. During this time it will move within an energy shell near the barrier top. The energy diffusion theory of Eq.(2.11) assumes that the trajectory will cross the saddle many times before being deactivated so that its position will be randomized[22] (see Fig. 2). It will then be deactivated on

either side of the transition state with equal probability. This leads to the multiplicative factor of $\frac{1}{2}$ for a symmetric system.

For a particular physical system, the internal properties of the potential and the external properties of the random force will determine the validity of this assumption. For a given potential, there will be an average time, τ_{TRAN} , for a trajectory to sample effectively all regions of the energy surface. This will be affected by the measure of irregular phase space in the isolated system which may contribute reactive trajectories [23], and the friction which may increase the measure of irregular trajectories. For a given friction, there will be an average time, τ_{ACT} , for which a trajectory energy remains in the region of the barrier with the possibility of crossing the transition state. The condition for the validity of Eq.(2.11) may then be expressed as $\tau_{\text{ACT}} \gg \tau_{\text{TRAN}}$. When $\tau_{\text{TRAN}} \gg \tau_{\text{ACT}}$ the activated trajectory will not have time to cover the full phase space and so there will be a reduced density of states contributing reactive trajectories and a reduced prefactor in Eq.(2.11).

A study of this effect has been made for the case of the BGK and strong collision models using a two-dimensional model potential[23]. Here, the particle is activated by a collision which thermalizes the momentum, or position and momentum, respectively. In each case, the majority of reacting trajectories are activated by a single collision and then move freely on an energy surface until being deactivated by the next collision. If the activated trajectory is in a region of phase space bounded by a KAM surface[65], which prevents it from crossing the transition state, it will never react[31,18]. Therefore,

for small collision frequencies, the rate constant for energy activation will be reduced by a factor which accounts for the portion of regular, non-reactive phase space.

For a weak collision model such as Eq.(2.10), a trajectory is activated by the continuous action of an infinitesimal random force which causes displacements in the position and momentum and therefore the energy. Contrary to the BGK and strong collision models, the activated trajectory's dynamics in the weak collision limit is not solely determined by the irregularity, or *intrinsic stochasticity*, of a particular energy surface. Once activated, the trajectory is still subject to these weak collisions and therefore undergoes transitions between adjacent energy surfaces. This mechanism of diffusion between energy surfaces, due to the external random force coupled to the internal diffusion on each particular energy surface, determines the *extrinsic stochasticity* of the system. The details of external random jumps in phase and action for the standard mapping has been studied in some detail[65]. In Sec. 5.6 we discussed a few mechanisms of extrinsic diffusion which may prove important and lead to quantitative differences between energy diffusion for the weak and strong collision models.

Experimental results for the isomerization of cyclohexane [49] have shown that as the pressure, or collision frequency, is increased there is a decrease in the slope of the rate constant as a function of pressure, or collision frequency. Recently, the many dimensional non-Markovian energy diffusion theory[117] has been used to interpret the experimental results[118]. It was decided,

from consideration of the isolated system, that the dimension of the reaction system was most probably six. This led to the conclusion that the maximum in the rate occurred in the gas phase, contrary to previous belief. Given our results, we question this conclusion. In particular, it is likely that while the low pressure behavior indicates a large number of dimensions contributing to the rate, at higher pressures a number of these dimensions may be eliminated leading to a decrease in the initial slope with increasing friction and a maximum rate predicted by a lesser dimensional theory. If the number of effective dimensions is reduced, from six at low pressures to three or less at high pressures, the maximum will occur in the liquid phase[118]. Recently Chandler, *et al.* have carried out BGK simulations.¹⁷ Their results corroborate our ideas.

¹⁷David Chandler, personal communication.

6 Non-Adiabatic Transitions

Our previous discussion has concentrated on a classical, adiabatic description of the reaction coordinate. It was assumed that (1) the temperature was high enough that tunneling was negligible in comparison with activated crossing of the barrier, and (2) the electronic state of the reacting molecule followed the motion of the nuclei adiabatically. The adiabatic potential surface corresponds to the ground state of the diagonalized Hamiltonian. These assumptions allow a simple description of nuclei moving on a Born-Oppenheimer potential surface according to Newton's equations of motion.

For those physical systems where the temperature is below a certain temperature, the "crossover temperature" [44], tunneling will be the dominant reaction channel and the first assumption will be violated[44]. The effect of a solvent on the tunneling frequency was first examined by Wolynes[115] and has since been given much attention. A recent review of this work is given by Hänggi[44]. Also, Pollak has unified many of these ideas under a single formalism, the multidimensional transition state theory[84].

For those systems whose temperature is above the crossover temperature, the dominant contribution to the rate should be activated barrier crossing. However, for those systems whose splitting between the excited and ground state adiabatic potential energy surfaces is small, the assumption of adiabatic curve crossing may be violated. For isolated systems, non-adiabatic effects have been incorporated in semi-classical trajectory calculations by Tully and

Preston[107], and Miller and George[74]. These ideas and further applications have been reviewed by Tully[106]. Recently, Cline and Wolynes have applied these techniques to study non-adiabatic effects in activated barrier crossing[57]. In this chapter, we review their work and present a statistical theory which accurately predicts their numerical results given the barrier crossing rate for the corresponding adiabatic system.

6.1 The Model of Cline and Wolynes

Cline and Wolynes examined a system consisting of a nuclear reaction coordinate, q , linearly coupled, by the parameter g , to a two-level system. The reaction coordinate moves in one of two electronic states which are modeled as harmonic wells centered at $q = \pm g$. The Hamiltonian is given by

$$H = \frac{1}{2}\dot{q}^2 + \frac{\omega^2}{2}q^2 + k\sigma_x + gq\sigma_z + H_B \quad (6.1)$$

where $\sigma_{x,z}$ are Pauli spin matrices, k is the matrix element which couples the two electronic states, and H_B is the bath Hamiltonian. The diabatic and adiabatic potential surfaces are shown in Fig. 18. The transition state surface is chosen at the curve crossing point $q = 0$ which has energy $Q = g^2/2$.

The bath was incorporated using a stochastic BGK model[19] which thermalizes the velocity of the reaction coordinate on each collision while sampling collision times from a Poisson distribution with average collision frequency ζ [56]. Within the adiabatic approximation, the rate constant at low friction is given by the result of Skinner and Wolynes, Eq. (2.12), while the

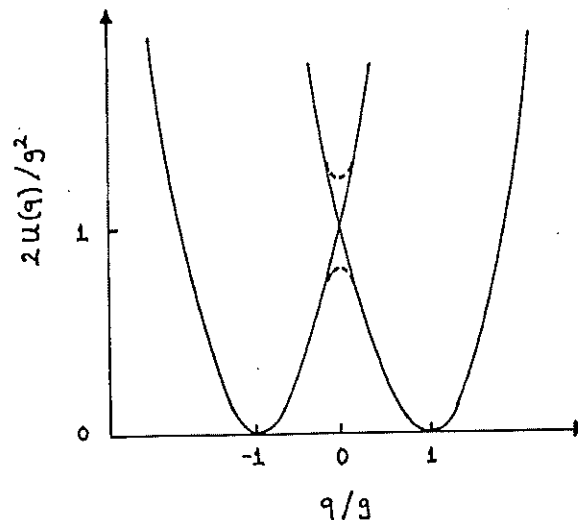


Figure 18: Potential surface for the Cline-Wolynes model.

high friction rate constant is given by the theory of Grote-Hynes, Eq. (2.13). The rate for all friction is then given by the connection formula, Eq. (2.18).

If the electronic state surfaces are strongly coupled, non-adiabatic effects are important. Cline and Wolynes used a surface hopping model to calculate non-adiabatic corrections to the adiabatic theory. They performed a trajectory calculation using the reactive flux formalism (Chap. 3); 10^4 trajectories were used for each rate constant calculation. Initially, those trajectories with $\dot{q} > 0$ were placed on the left diabatic surface (Fig. 18) while those trajectories with $\dot{q} < 0$ were on the right diabatic surface. The trajectories begin at the transition state $q = 0$ and then are propagated on the diabatic surface according to the BGK algorithm until they recross the transition state, at which point the probability of hopping to the other diabatic surface is calculated. The trajectory is then either moved to the other diabatic surface, or continues on the present surface. Trajectories with initial velocity $\dot{q} > 0$

are immediately tested for curve crossing (as though they had started just to the left of the transition state) while those with initial velocity $\dot{q} < 0$ are moved away from the surface and are only tested for crossing on return (as though they had started just to the left of the transition state).

The probability for curve crossing on a single passage through the curve crossing region is given approximately by the Landau-Zener-Stueckelberg formula[106,52]

$$P_{LZS} = 1 - e^{-2\pi k^2/\hbar v|F_2-F_1|} \quad (6.2)$$

where $F_{1,2}$ are the slopes of the diabatic potential surfaces at the point of curve crossing and v is the velocity of the trajectory at the point of curve crossing. Note that for small velocities, where the nuclei move very slowly, the probability of curve crossing will approach unity and the reaction coordinate will move on the adiabatic Born-Oppenheimer surface.

Results for the BGK simulation of Cline and Wolynes are given in Table 1 for the two non-adiabatic calculations and their corresponding adiabatic systems.¹⁸ The parameters defining system 1 (2), chosen to approximate ligand binding to hemoproteins[57], in units of $\hbar\omega$, are $k = 0.3(4243)$, $g = 1.87(4.1195)$, and $\beta Q = 21.0(4.0)$. The adiabatic rate constants agree well with the theory of Skinner and Wolynes, Eq. (2.12), at low collision frequency and with the spatial diffusion rate constant for a cusped barrier, Eq. (2.17), at high collision frequency.

¹⁸We thank Raymond Cline and Peter Wolynes for providing us with this data.

Table 1: BGK simulation results for the transmission coefficient $\kappa = k/k_{TST}$ as a function of collision frequency, ζ .

ζ	Adiabatic	System 1	Adiabatic	System 2
0.00	0.0000	0.0000	0.0000	0.0000
0.05	0.1211	0.1298	0.0906	0.0693
0.10	0.2703	0.2351	0.2036	0.1382
0.20	0.4661	0.3545	0.3426	
0.30	0.6857	0.4562	0.5527	
0.40	0.7874	0.5290	0.6363	
0.50	0.8677	0.5516	0.7391	0.1713
1.00	0.9344	0.5331	0.8471	0.1734
1.50	0.9081	0.5194	0.8478	0.1716
2.00	0.8870	0.5275	0.7372	0.1758
3.50	0.8000	0.4817	0.5879	0.1306
5.00	0.7275	0.4624	0.4767	0.1328
7.00	0.6362	0.4122	0.3730	0.1316
10.00	0.5443	0.3715	0.2815	0.1406
15.00	0.4062	0.3141	0.2049	0.1049
30.00	0.2460	0.2054	0.1107	0.0714

The non-adiabatic rate constants agree with the qualitative discussion presented by Cline and Wolynes. In particular, the maximum in the rate is given approximately by

$$k_{MAX} \approx \bar{P}_{LZS} k_{TST} \quad (6.3)$$

where \bar{P}_{PLZ} is the average curve crossing probability for a trajectory crossing the transition state.¹⁹

¹⁹Cline and Wolynes approximate \bar{P}_{LZS} by replacing v in Eq. (6.2) with the average velocity of the Maxwell distribution. A more accurate approximation is to replace v with the average velocity of the weighted distribution, Eq. (3.6), corresponding to those trajectories crossing the transition state surface.

6.2 Our Theory

Here, following, we apply the absorbing boundary formalism (Chap. 3) to the system of Cline and Wolynes. We only assume 1) that the distribution of those states recrossing the transition state is given by the equilibrium distribution, Eq. (3.6), and 2) that the velocity dependent probability for curve crossing, Eq. (6.2), can be replaced by its average value \bar{P}_{LZS} . For high barriers, the velocity probability distribution function for trajectories crossing the transition state surface, is strongly peaked and the average curve crossing probability is well approximated by Eq. (6.2), where $v = (k_B T / \mu)^{1/2}$ where μ is the reduced mass of the reaction coordinate. We restrict ourselves to a discussion of symmetric double wells.

The reactive flux is given by Eq. (3.5) in terms of the averages $\langle \theta[x(t)] \rangle_{\pm}$ which are the fraction of trajectories in the product well which begin at the transition state with initial velocity $\pm \dot{q} > 0$. We would like to calculate the transmission coefficient, $\kappa = k/k_{TST}$. We assume that there are two types of trajectories, those which move into the wells and are trapped for long times and those which rebound from the turning point of the potential, or are reversed by collisions, and recross the transition state in a short time. This assumption is that of a separation of time scales necessary for a plateau in the reactive flux (Chap. 3).

To begin, we define some useful quantities. Consider those trajectories with initial velocity $\dot{q} > 0$ which are on the left diabatic surface immediately

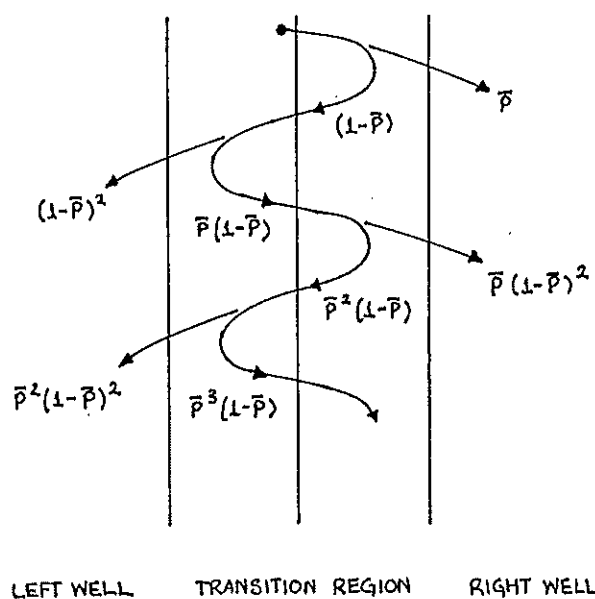


Figure 19: Schematic diagram for the calculation of α and β where $\bar{P} \equiv \bar{P}_{LZS}$.

to the left of the transition state (Fig. 19).²⁰ Moving to the right, they immediately cross the transition state and are given the opportunity to cross curves so that a fraction, \bar{P}_{LZS} , immediately cross onto the right diabatic surface into the well region, while $1 - \bar{P}_{LZS}$ reach the turning point of the left diabatic surface and return to the transition state. Of those trajectories returning to the transition state, having $\dot{q} < 0$, a fraction $1 - \bar{P}_{LZS}$ will remain on the left diabatic surface and move into the left well. The complementary fraction \bar{P}_{LZS} will cross onto the right diabatic surface, reach its turning point, and return to the transition state where trajectories may cross curves or move into the right well. Further, the total fraction of trajectories initiated

²⁰These trajectories are in the transition region which corresponds to the excited state adiabatic potential surface. In the limit of low velocities, where $\bar{P}_{LZS} \approx 1$, trajectories may remain on this excited state surface for very long times by repeatedly crossing curves.

just to the left of the transition state, having velocity $\dot{q} > 0$, which move from the transition region into the right well is given by

$$\alpha = \frac{2\bar{P}_{LZS}}{1 + \bar{P}_{LZS}} \quad (6.4)$$

while the fraction which reach the left well is given by

$$\beta = 1 - \alpha = \frac{1 - \bar{P}_{LZS}}{1 + \bar{P}_{LZS}}. \quad (6.5)$$

To include the effects of activated barrier crossing, we define T_o which is the probability that a trajectory crossing the transition state and moving into a well will be trapped in that well for long times before recrossing the transition state (see Chap. 3). Using these quantities, we now calculate $\langle \theta[x(t)] \rangle_{\pm}$.

The scheme of Cline and Wolynes dictates that those trajectories forming the average $\langle \theta[x(t)] \rangle_+$ begin slightly to the left of the transition state on the left diabatic surface with $\dot{q} > 0$ (Fig. 20). After some time, a fraction α will move into the right well while a fraction β will move into the left well. Of those trajectories moving into the right well, a fraction T_o will be trapped for a long time while $1 - T_o$ return to the transition region. Of those trajectories which return to the transition region from the right well, having $\dot{q} < 0$, a fraction β will move back into the right well while a fraction α will move into the left well. It follows that the fraction of trajectories which are trapped in the right well having never recrossed the transition state is αS_o , where

$$S_o = \frac{T_o}{1 - \beta(1 - T_o)} \quad (6.6)$$

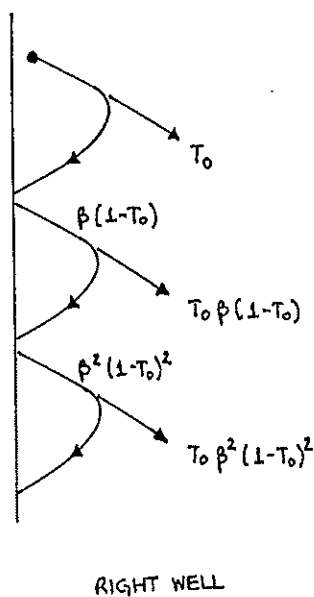


Figure 20: Schematic diagram for the calculation of S_o .

is the probability of being trapped in the right well, having started on the right diabatic surface moving out of the transition region with $\dot{q} > 0$, while never passing through the transition region into the left well.

The total fraction of trajectories initially leaving the transition region moving into the right well which then recross the transition state, curve crossing to the left diabatic surface, and become trapped in the left well is $S_o(1 - S_o)$. The fraction that recross the transition state twice and become trapped in the right well is $S_o(1 - S_o)^2$, and so on (Fig. 21). It follows that the total fraction of trajectories which are trapped in the right well, having initially moved out of the transition region into the right well, added to those trajectories trapped in the right well which initially moved out of

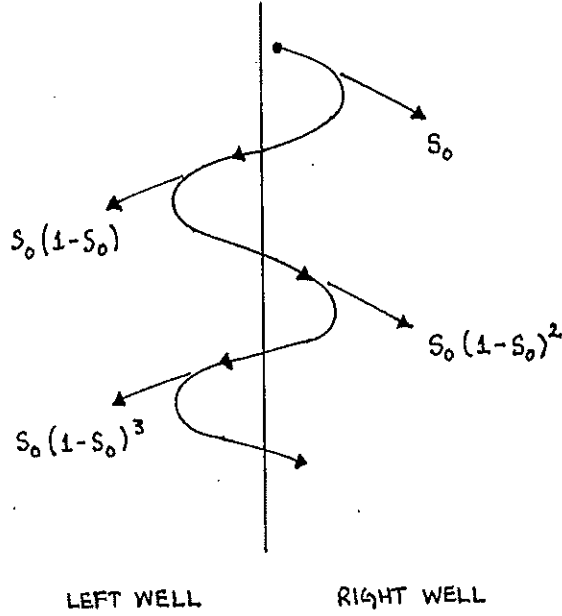


Figure 21: Schematic diagram for the calculation of $\langle \theta[x(t)] \rangle_+$.

the transition region into the left well is

$$\langle \theta[x(t)] \rangle_+ = \frac{\alpha S_0}{1 - (1 - S_0)^2} + \frac{\beta S_0(1 - S_0)}{1 - (1 - S_0)^2} = \frac{1 - \beta S_0}{2 - S_0}. \quad (6.7)$$

Those trajectories forming the average $\langle \theta[x(t)] \rangle_-$ begin slightly to the left of the transition state on the left diabatic surface, with $\dot{q} < 0$. The trajectories then move out of the transition region into the left well where a fraction T_0 will be trapped for a long time while $1 - T_0$ return to the transition region. Of those trajectories which return to the transition region from the left well, having $\dot{q} > 0$, a fraction α move back into the right well while a fraction β move into the left well. It follows that the total fraction of trajectories which are trapped in the right well having initial velocity $\dot{q} < 0$ is

$$\langle \theta[x(t)] \rangle_- = \frac{S_0(1 - S_0)}{1 - (1 - S_0)^2} = \frac{1 - S_0}{2 - S_0}. \quad (6.8)$$

The transmission coefficient is

$$\kappa = \frac{k_f + k_b}{k_{TST}} = \frac{\alpha S_o}{2 - S_o}. \quad (6.9)$$

In the adiabatic limit, $\bar{P}_{LZS} = 1$, $\alpha = 1$, $\beta = 0$, $S_o = T_o$, and $\kappa = T_o/(2 - T_o)$ which is the transmission coefficient found in our previous adiabatic analysis, Eq. (3.17). In the strongly non-adiabatic limit, for $T_o \gg \bar{P}_{LZS}$, $\kappa \approx \alpha$ while for $T_o \ll \bar{P}_{LZS}$, $\kappa \approx T_o/2$ which is the asymptotic adiabatic result for small T_o . The largest deviations from the adiabatic theory should occur for intermediate collision frequency where the maximum in the rate constant is reduced by non-adiabatic effects.

Notice that the maximum in our transmission coefficient for a given \bar{P}_{LZS} is found for $T_o = 1$ where $\kappa = \alpha$ and $k = \alpha k_{TST}$, while Cline and Wolynes propose that the rate constant should show a maximum of $k = \bar{P}_{LZS} k_{TST}$. The simulation results in Table 1 show a maximum in the transmission coefficient of the diabatic rate data of approximately .552 (.176) for system 1 (2). An accurate calculation of \bar{P}_{LZS} produces .407 (.090) which, when combined with Eq. (6.4), corresponds to an α of .578 (.165). Therefore, our estimate of the maximum in the transmission coefficient is more accurate than the estimate of Cline and Wolynes, showing better agreement with their simulation results.

6.3 Comparison

It is straightforward to apply Eq. (6.9). Given the adiabatic rate constant, one may extract the trapping coefficient T_o using

$$T_o = \frac{2\kappa}{1 + \kappa}. \quad (6.10)$$

The rate constant for any corresponding non-adiabatic system may then be found by calculating the average curve crossing probability, \bar{P}_{LZS} , using Eq. (6.2) for the appropriate system parameters and substituting T_o and \bar{P}_{LZS} into Eqs. (6.4), (6.5), (6.6), and (6.9).

In Fig. 22 we compare the predictions of Eq. (6.9) with the simulation data of Cline and Wolynes. The adiabatic prediction (—) is calculated using the theory of Skinner and Wolynes, Eq.(2.12), at low collision frequency, ζ , and the spatial diffusion rate constant for a cusped barrier, Eq. (2.17), at large ζ ; the non-adiabatic results (— —) follow from Eq. (6.9) while the simulation results are shown for the adiabatic (o) and non-adiabatic (•) reactive flux calculations of Cline and Wolynes for a) system 1 and b) system 2. The agreement is excellent, indicating that our model accurately represents the dynamics of the stochastic simulation. The question of the physical validity of the model of Cline and Wolynes will be discussed in the section which follows.

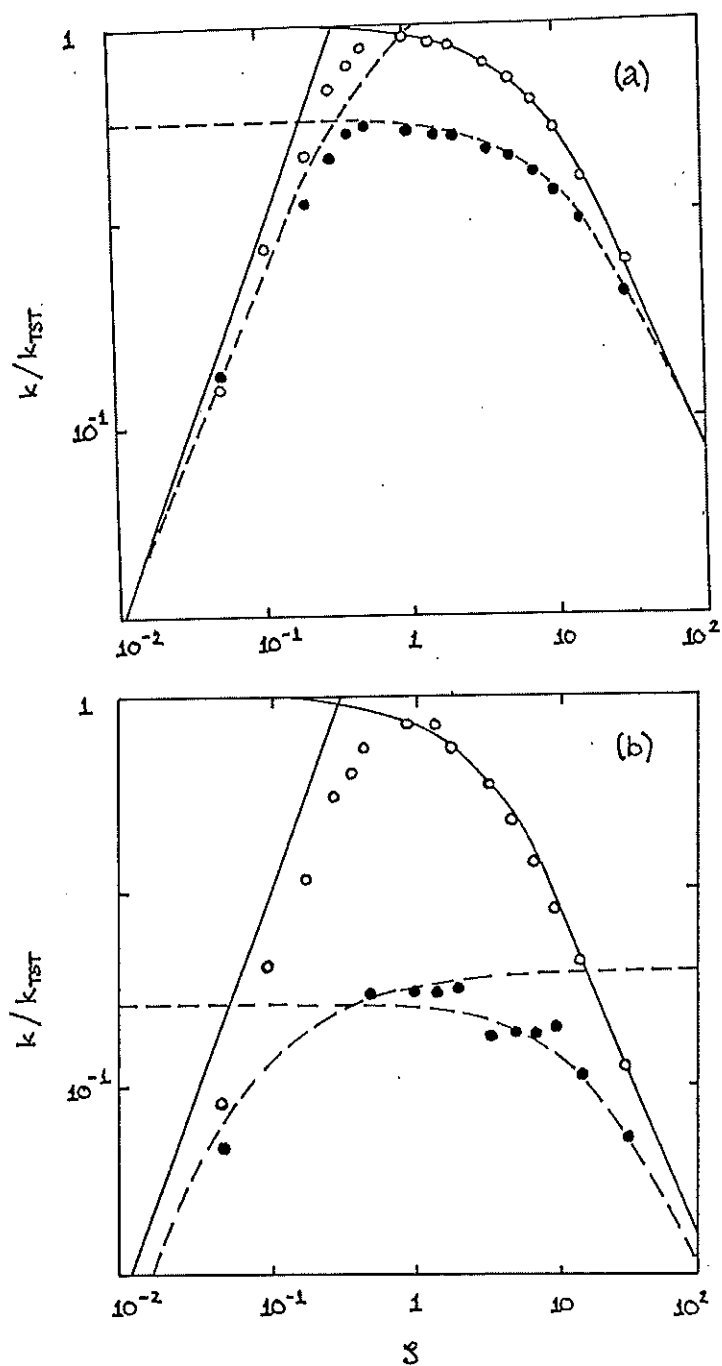


Figure 22: Our theory compared to the simulation results of Table 1.

6.4 Discussion

While our model accurately predicts the simulation results, it is unclear whether the model of Cline and Wolynes, while an excellent first step, is a realistic one for measuring non-adiabatic curve crossing effects on activated barrier crossing. Below we focus on a number of specific problems.

1) The Landau-Zener-Stueckelberg theory assumes that the velocity of particles in the curve crossing region is constant, or that the excess kinetic energy is large. This assumption is certainly a bad one for barrier crossing with reasonably high barriers. The average energy of those states crossing the barrier will be close to the barrier energy, with the average kinetic energy being $k_B T$. It is likely that the barrier maximum will be located at the point of curve crossing which will be very close to the turning points of the diabatic surfaces. The constant velocity assumption of the Landau-Zener-Stueckelberg theory should be very poor.

2) The classical trajectory method also assumes that there are no interference effects for trajectories which remain in the excited state and oscillate for long times. Child has calculated the probability of curve crossing for the case when the slopes of the diabatic surfaces at the point of crossing, F_1 and F_2 , are of opposite sign. He finds that interference effects can be important[29]. Cline and Wolynes recognize this and have proposed a quantum mechanical model which attempts to include interference effects important in the crossing region [57]. Also, note that the Landau-Zener-Stueckelberg calculation is asymptotic in time. It involves the calculation of the probability that a

wavefunction, initially at $q = +\infty$, will be at $q = -\infty$ at $t = +\infty$. In this application, the double well potential leads to bound states where the asymptotic limits used to separate states are not appropriate.

3) The choice of initial conditions for the reactive flux calculation is somewhat arbitrary. It is not clear why the reactants and products have been separated spatially, to the right or left of the transition state, rather than according to which diabatic surface they reside on. The spatial separation, while an obvious extension of the reactive flux formalism, is ambiguous during the transient period when trajectories spend time in the transition region.

4) The connection formula proposed by Hynes, Eq. (2.18), can be understood as the sum of times for energy activation to the barrier energy and spatial diffusion through the barrier region. This model for electronic curve crossing has a cusped barrier and therefore lacks distinct well and barrier regions. The rate constant for spatial diffusion with a cusped barrier, Eq. (2.17), is the inverse mean passage time for traveling from the reactant well minimum to the minimum of the product well[62]. Therefore, because of the overlap in regions of spatial and energy diffusion, the time for energy activation added to the time for spatial diffusion from one well minimum to the other would overestimate the total time and underestimate the total rate constant and Eq. (2.18) cannot be applied to problems involving cusped barriers.

7 Conclusion

We have presented an approximate method for calculating reaction rate constants for activated barrier crossing, the absorbing boundary method. We were able to examine a number of physically distinct models for chemical reaction systems and study the validity of existing theoretical predictions for these systems. In addition, the formalism used to calculate the absorbing boundary rate constant proved useful in developing a statistical theory which incorporates non-adiabatic effects in activated barrier crossing.

7.1 Is Transition State Theory Enough?

We have tried to indicate how this method may be applied to stochastic simulation. Recently, we have applied the absorbing boundary method to the calculation of rate constants for a diatomic molecule, moving in a bistable potential, solvated in a Lennard-Jones fluid. Our results indicate that at low densities impulsive collision models may give a more accurate representation of the dynamics than the weak collision generalized Langevin equation. At high density we find that it is difficult to produce frictions which lead to large deviations from transition state theory.

In any case, for most reacting molecules at low friction the reaction coordinate is strongly coupled to several internal degrees of freedom leading to an energy activation rate which increases quickly as a function of friction (see Eq. (2.11)). This restricts the energy activation regime to very low collision frequency so that it is difficult to measure experimentally[14,76]. Of course,

if some of the non-reactive modes are strongly coupled to the solvent it is possible that they will become overdamped and may be eliminated (Chap. 5) reducing the size of the reaction system and the energy activation rate. Nevertheless, the large number of degrees of freedom of most systems, added to the difficulty of finding solvents which strongly damp the reaction coordinate, implies that transition state theory may be a good estimate of the rate constant for many experimental systems over a wide range of friction. Recent computer experiments indicate that this is the case for $A + BC$ reactions in rare gas solution[13].

While substantial deviations from transition state theory for large molecular systems may be difficult to find, small deviations abound. Experiments on the isomerization of 1,1' binaphthyl[73] and stilbene[68,37,64] each show a rate reduced by an order of magnitude from the transition state theory value. Also, recent computer experiments using the absorbing boundary method have shown an order of magnitude reduction in the rate of rotational isomerization for the tyrosine 35 sidechain in aqueous bovine pancreatic trypsin inhibitor[38]. This simulation, while freezing out many modes, consisted of 306 protein atoms and 162 water molecules.

7.2 Biomolecular Systems

These results are an indication of the size of dynamic calculation which is presently feasible. With the proliferation of supercomputers and fast vector processing techniques[113] it has become possible to study large molecular systems of biological interest. Protein conformational transitions[10,33,59]

and enzyme substrate reactions[101,95,77] are particularly ripe for study. For instance, the passage of a K^+ ion through the membrane channel of solvated gramicidin A has been well characterized using energy minimization[35], Monte Carlo[61], and fits of transition state theory to experimental data[34]. It would be interesting to study the dynamics of the ion passage using more accurate rate theories (Chap. 2) and numerical simulation (Chap. 3).

In the Marcus theory of intermolecular electron transfer between, for example, cytochrome c oxidase and reductase[69,20,103], a number of parameters must be experimentally determined or modeled. These include the mean square separation of the charge transfer centers, dielectric constants of the surrounding protein and solvent, radii of the reactants, as well as force constants and bond lengths, and conformational changes preceding and following the electron transfer[71]. The separations and orientation of charge transfer centers are experimentally accessible. Recent calculations of electron transfer rates have indicated the need for more accurate data on solvent reorientational contributions to the free energy of oxidation[71]. In addition, more detailed information on steric factors which account for nonspherical charge transfer probability would be useful as these factors are only crudely approximated for complex systems.

Theories of electron transfer require an estimate of the probability for achieving a certain nuclear separation of the charge transfer centers. As we have seen, this probability can deviate from the transition state theory estimate. For systems at high temperatures, a classical trajectory analysis

of such systems could provide information on the rate at which the nuclei achieve the reactive separation and the solvent effects on that rate. In addition, our theory for the calculation of non-adiabatic effects on reaction rates (Chap. 6) could provide information on the reduction in rate due to non-adiabatic transitions.

7.3 Small Molecules and Models

In addition to biochemical systems, smaller chemical reaction systems deserve more attention both theoretically and experimentally. The assumption of chaotic motion for many dimensional systems in the low friction limit should be further examined[89,48]. Recently, calculations on a two-dimensional reaction system using the impulsive BGK collisional model have shown large reductions in the rate for energy activation when the assumption of fast equipartitioning between vibrational modes is violated[23]. For this collision model, it was found that the absorbing boundary formalism (Chap. 3) could be extended to predict rate constants for *any* collision frequency given only the survival probability function $P(t)$ of the *isolated* system.

Interest should also be taken in resolving the current controversy over whether non-Markovian effects are important in real chemical systems. Bagchi and Oxtoby found that the theory of Grote and Hynes[54] could explain deviations from Kramers' theory for the experimentally measured isomerization rate of diphenyl butadiene[9]. Since that time, Hochstrasser and coworkers, following the ideas of Velsko, Waldeck, and Fleming [111], have shown that Kramers' theory can fit this data if the zero frequency friction

parameter is derived from the rotational relaxation time rather than the bulk solvent viscosity[63]. Experiments which vary the internal structure of the solvent, as well as its mass and size, should provide important information.

It would be useful to examine the assumptions implicit in relating rotational relaxation times to the friction experienced by the reaction coordinate. A molecular dynamics computer simulation of n-butane in a Lennard-Jones solvent could provide the rotational relaxation time of the whole molecule as well as the memory function for the dihedral angle, the reaction coordinate for the trans-gauche isomerization. Results at various densities could be compared to examine the correlation between the zero frequency friction and the rotational relaxation time. Additionally, it has been suggested that the proper rotational relaxation time to be used in the isomerization of 1,1'-binaphthyl would be that of naphthalene rather than the whole molecule.²¹ By extending the calculation discussed above, numerically calculating the rotational relaxation time for ethane in the Lennard-Jones solvent, this suggestion could be theoretically tested.

²¹Kenneth Eisenthal, personal communication.

References

- [1] *APMATH64 Manual*. Floating Point Systems, (1983).
- [2] M. Abramowitz and I. A. Stegun. *Handbook of Mathematical Functions*. Dover, New York, NY, (1964).
- [3] J. E. Adams and J. D. Doll. *J. Chem. Phys.*, 80:1681, (1984).
- [4] S. A. Adelman. *Adv. Chem. Phys.*, 53:61, (1983).
- [5] B. J. Alder and T. E. Wainwright. *J. Chem. Phys.*, 31:459, (1959).
- [6] M. P. Allen and P. Schofield. *Mol. Phys.*, 39:207, (1980).
- [7] J. B. Anderson. *J. Chem. Phys.*, 58:4684, (1973).
- [8] V. I. Arnold. *Ordinary Differential Equations*. MIT, Cambridge, MA, (1985).
- [9] B. Bagchi and D. A. Oxtoby. *J. Chem. Phys.*, 78:2735, (1983).
- [10] D. Beece, L. Eisenstein, H. Frauenfelder, D. Good, M. C. Marden, L. Reinisch, A. H. Reynolds, L. B. Sorensen, and K. T. Yue. *Biochem.*, 19:5147, (1980).
- [11] C. H. Bennett. In R. E. Christofferson, editor, *Algorithms for Chemical Computation*, American Chemical Society, Washington, DC, (1977).
- [12] D. Bensimon and L. P. Kadanoff. *Physica*, 13D:82, (1984).
- [13] J. P. Bergsma, J. R. Reimers, K. R. Wilson, and J. T. Hynes. Molecular dynamics of the $a + bc$ reaction in rare gas solution. (preprint).
- [14] B. J. Berne. *Chem. Phys. Lett.*, 107:131, (1984).
- [15] B. J. Berne. In J. U. Brackbill and B. I. Cohen, editors, *Multiple Time Scales*, Academic Press, New York, NY, (1985).

- [16] B. J. Berne, J. P. Boone, and S. A. Rice. *J. Chem. Phys.*, 45:1086, (1966).
- [17] B. J. Berne, M. Borkovec, and J. E. Straub. Classical and novel methods in reaction rate theory and simulation. Feature article, submitted to *J. Phys. Chem.*
- [18] B. J. Berne, N. DeLeon, and R. O. Rosenberg. *J. Phys. Chem.*, 86:2166, (1982).
- [19] P. L. Bhatnagar, E. P. Gross, and R. M. Krook. *Phys. Rev.*, 94:511, (1954).
- [20] L. A. Blumenfeld, R. M. Davydov, N. S. Fel, S. N. Magonov, and R. O. Vilu. *FEBS Lett.*, 45:256, (1974).
- [21] M. Borkovec. Doctoral thesis, Columbia University. 1986.
- [22] M. Borkovec and B. J. Berne. *J. Chem. Phys.*, 82:794, (1985).
- [23] M. Borkovec, J. E. Straub, and B. J. Berne. *J. Chem. Phys.*, 85:146, (1986).
- [24] B. Carmeli and A. Nitzan. *Phys. Rev. Lett.*, 49:423, (1982).
- [25] B. Carmeli and A. Nitzan. *Chem. Phys. Lett.*, 106:329, (1984).
- [26] B. Carmeli and A. Nitzan. *J. Chem. Phys.*, 80:3596, (1984).
- [27] C. Cerjan and W. P. Reinhardt. *J. Chem. Phys.*, 71:1819, (1979).
- [28] D. Chandler. *J. Chem. Phys.*, 68:2959, (1978).
- [29] M. S. Child. *Molecular Collision Theory*. Academic Press, New York, NY, (1974).
- [30] P. Debye. *Trans. Electrochem. Soc.*, 82:265, (1942).

- [31] N. DeLeon and B. J. Berne. *J. Chem. Phys.*, 75:3495, (1981).
- [32] G. Van der Zwan and J. T. Hynes. *J. Chem. Phys.*, 77:1295, (1982).
- [33] V. Doster. *Biophys. Chem*, 17:97, (1983).
- [34] G. Eisenman and J. P. Sandblom. *Biophys. J.*, 45:88, (1984).
- [35] C. Etchebest and A. Pullman. *J. Bio. Struct. Dyn.*, 3:805, (1986).
- [36] H. Eyring. *J. Chem. Phys.*, 3:107, (1934).
- [37] G. R. Fleming, S. H. Courtney, and M. W. Balk. *J. Stat. Phys.*, 42:83, (1986).
- [38] I. Ghosh and J. A. McCammon. Sidechain rotational isomerization in proteins: Dynamic simulation with solvent surroundings. (preprint).
- [39] R. F. Grote and J. T. Hynes. *J. Chem. Phys.*, 73:2715, (1980).
- [40] R. F. Grote and J. T. Hynes. *J. Chem. Phys.*, 77:3736, (1982).
- [41] R. F. Grote and J. T. Hynes. *J. Chem. Phys.*, 74:4465, (1981).
- [42] H. Haken. *Synergetics*. Springer, New York, NY, (1983).
- [43] P. Hänggi. In W. Horsthemke and D. K. Kondepudi, editors, *Fluctuations and Sensitivity in Nonequilibrium Systems*, Springer, New York, NY, (1984).
- [44] P. Hänggi. *J. Stat. Phys.*, 42:105, (1985). Addendum and Erratum, *ibid.*, 44:1003, (1986).
- [45] P. Hänggi, H. Grabert, G. L. Ingold, and U. Weiss. *Phys. Rev. Lett.*, 55:761, (1985).
- [46] P. Hänggi and F. Mojtabai. *Phys. Rev. A*, 26:1168, (1982).

- [47] P. Hänggi and U. Weiss. *Phys. Rev. A*, 29:2265, (1984).
- [48] W. L. Hase. In W. H. Miller, editor, *Dynamics of Molecular Collisions, Part B.*, Plenum Press, New York, NY, (1976).
- [49] D. L. Hasha, T. Eguchi, and J. Jonas. *J. Am. Chem. Soc.*, 104:2290, (1982).
- [50] J. Hicks, M. Vandersall, Z. Babarogic, and K. Eisenthal. *Chem. Phys. Lett.*, 116:18, (1985).
- [51] H. Hippler, V. Schubert, and J. Troe. *J. Chem. Phys.*, 81:3931, (1984).
- [52] D. M. Hirst. *Potential Energy Surfaces - Molecular Structure and Reaction Dynamics.* Taylor and Francis, Philadelphia, PA, (1985).
- [53] J. T. Hynes. *Ann. Rev. Phys. Chem.*, 36:573, (1985).
- [54] J. T. Hynes. In M. Baer, editor, *Theory of Chemical Reaction Dynamics*, page 171, CRC Press, Boca Raton, FL, (1985).
- [55] J. T. Hynes, R. Kapral, and M. Weinberg. *J. Chem. Phys.*, 69:2725, (1978).
- [56] J. A. Montgomery Jr., D. Chandler, and B. J. Berne. *J. Chem. Phys.*, 70:4056, (1979).
- [57] R. E. Cline Jr. and P. G. Wolynes. Stochastic dynamic model of curve crossing phenomena in condensed phases. (preprint).
- [58] M. Kalos and P. A. Whitlock. Monte carlo methods and simulation of physical systems. (unpublished).
- [59] M. Karplus and J. A. McCammon. *Ann. Rev. Biochem.*, 53:263, (1983).
- [60] J. C. Keck. *Adv. Chem. Phys.*, 13:85, (1967).

- [61] K. S. Kim, D. P. Vercauteren, M. Welti, S. Chin, and E. Clementi. *Biophys. J.*, 47:327, (1985).
- [62] H. A. Kramers. *Physica*, 7:284, (1940).
- [63] M. Lee, A. J. Bain, P. J. McCarthy, C. H. Han, J. N. Haseltine, III, A. B. Smith, and R. M. Hochstrasser. *J. Chem. Phys.*, 85:4341, (1986).
- [64] M. Lee, G. R. Holtom, and R. M. Hochstrasser. *Chem. Phys. Lett.*, 118:359, (1985).
- [65] A. J. Lichtenberg and M. A. Lieberman. *Regular and Stochastic Motion*. Springer, New York, NY, (1983).
- [66] R. S. MacKay, J. D. Meiss, and I. C. Percival. *Physica*, 13D:55, (1984).
- [67] B. H. Mahan. *College Chemistry*. Addison-Wesley, Reading, MA, (1966).
- [68] G. Maneke, J. Schroeder, J. Troe, and F. Voß. *Ber. Bun. Phys. Chem.*, 89:896, (1985).
- [69] B. Mao, M. R. Pear, J. A. McCammon, and S. H. Northrup. *Biopolymers*, 21:1979, (1982).
- [70] F. Marchesoni and P. Grigolini. *J. Chem. Phys.*, 78:6287, (1983).
- [71] R. A. Marcus and N. Sutin. *Biochim. et Biophys. Acta*, 811:265, (1985).
- [72] N. Metropolis, A. W. Rosenbluth, M. N. Rosenbluth, A. H. Teller, and E. Teller. *J. Chem. Phys.*, 21:1087, (1953).
- [73] D. P. Millar and K. B. Eisenthal. Picosecond dynamics of barrier crossing in solution: A study of the conformational change of excited state 1, 1' - binaphthyl. (preprint).
- [74] W. H. Miller and T. F. George. *J. Chem. Phys.*, 56:5637, (1972).

- [75] H. Mori. *Prog. Theor. Phys.*, 33:423, (1965).
- [76] A. Nitzan. *J. Chem. Phys.*, 82:1614, (1985).
- [77] S. H. Northrup, S. A. Allison, and J. A. McCammon. *J. Chem. Phys.*, 80:1517, (1984).
- [78] S. H. Northrup and J. T. Hynes. *J. Chem. Phys.*, 73:2700, (1980).
- [79] S. Okuyama and D. Oxtoby. *J. Chem. Phys.*, 84:5824, (1986).
- [80] S. Okuyama and D. Oxtoby. *J. Chem. Phys.*, 84:5830, (1986).
- [81] L. Onsager. *Phys. Rev.*, 54:554, (1938).
- [82] B. Otto, J. Schroeder, and J. Troe. *J. Chem. Phys.*, 81:202, (1984).
- [83] P. Pechukas. In W. H. Miller, editor, *Dynamics of Molecular Collisions, Part B.*, Plenum Press, New York, NY, (1976).
- [84] E. Pollak. *Phys. Rev. A*, 33:4244, (1986).
- [85] E. Pollak. *J. Chem. Phys.*, 85:865, (1986).
- [86] A. Rahman. *Phys. Rev.*, 136:A405, (1964).
- [87] D. W. Rebertus, B. J. Berne, and D. Chandler. *J. Chem. Phys.*, 70:3395, (1979).
- [88] W. P. Reinhardt. *J. Phys. Chem.*, 86:2158, (1982).
- [89] O. K. Rice. *Z. Phys. Chem. B*, 7:226, (1930).
- [90] R. O. Rosenberg, B. J. Berne, and D. Chandler. *Chem. Phys. Lett.*, 75:162, (1980).
- [91] R. O. Rosenberg, R. Mikkilineni, and B. J. Berne. *J. Am. Chem. Soc.*, 104:7647, (1982).

- [92] B. D. Ross and N. S. True. *J. Am. Chem. Soc.*, 105:1382, (1983).
- [93] B. D. Ross and N. S. True. *J. Am. Chem. Soc.*, 105:4871, (1983).
- [94] J. Schroeder and J. Troe. *Chem. Phys. Lett.*, 116:453, (1985).
- [95] D. Shoup, G. Lipari, and A. Szabo. *Biophys. Jour.*, 36:697, (1981).
- [96] S. J. Singer, R. A. Kuharski, and David Chandler. (preprint).
- [97] J. L. Skinner and P. G. Wolynes. *J. Chem. Phys.*, 72:4913, (1980).
- [98] J. L. Skinner and P. G. Wolynes. *J. Chem. Phys.*, 69:2143, (1978).
- [99] N. B. Slater. *Theory of Unimolecular Reactions*. Cornell University Press, Ithaca, NY, (1959).
- [100] M. Smoluchowski. *Z. Phys. Chem.*, 92:129, (1918).
- [101] K. Sölc and W. H. Stockmayer. *I. Jour. Chem. Kin.*, 5:733, (1973).
- [102] W. C. Swope, H. C. Andersen, P. H. Berens, and K. R. Wilson. *J. Chem. Phys.*, 72:4350, (1980).
- [103] T. Takano and R. E. Dickerson. *J. Mol. Biol.*, 153:95, (1981).
- [104] S. Toxvaerd. *J. Chem. Phys.*, 82:5658, (1985).
- [105] D. G. Truhlar, W. L. Hase, and J. T. Hynes. *J. Phys. Chem.*, 87:2664, (1983).
- [106] J. C. Tully. In W. H. Miller, editor, *Dynamics of Molecular Collisions, Part B.*, Plenum Press, New York, NY, (1976).
- [107] J. C. Tully and R. K. Preston. *J. Chem. Phys.*, 55:562, (1971).
- [108] P. Turq, F. Lantelme, and H. L. Friedman. *J. Phys. Chem.*, 66:3039, (1977).

- [109] J. P. Valleau and S. G. Whittington. In B. J. Berne, editor, *Statistical Mechanics, Part A.*, Plenum Press, New York, NY, (1976).
- [110] G. van der Zwan and J. T. Hynes. *J. Chem. Phys.*, 76:2993, (1982).
- [111] S. P. Velsko, D. H. Waldeck, and G. R. Fleming. *J. Chem. Phys.*, 78:249, (1983).
- [112] P. B. Visscher. *Phys. Rev. B*, 13:3272, (1976).
- [113] A. Wallqvist. Doctoral thesis, Columbia University. 1986.
- [114] E. Wigner. *J. Chem. Phys.*, 5:720, (1937).
- [115] P. G. Wolynes. *Phys. Rev. Lett.*, 47:968, (1981).
- [116] T. Yamamoto. *J. Chem. Phys.*, 33:281, (1960).
- [117] A. G. Zawadzki and J. T. Hynes. *Chem. Phys. Lett.*, 113:476, (1985).
- [118] A. G. Zawadzki and J. T. Hynes. Vibrational energy transfer and isomerization reactions in solution. (preprint).
- [119] R. Zwanzig. *Phys. of Fluids*, 2:12, (1959).

Appendix

The following is a brief outline of how one can apply the absorbing boundary method to calculate rate constants. The quantities we are interested in calculating are the survival probabilities $P_{\pm}(t)$ which are simply the number of trajectories initially entering the (-) reactant or (+) product well which remain in the well, having not crossed the transition state, after time t , Sect. (3.2). One must average from 10^2 to 10^4 trajectories to obtain reasonable accuracy; the exact number will depend on the particular problem. Like most molecular dynamics calculations, the absorbing boundary method may be readily vectorized[113].

1) *Choose the initial conditions.* The initial distribution of states corresponds to

$$P^{(\pm)}(\Gamma) = \frac{\dot{x}\theta(\pm\dot{x})\delta(x)e^{-\beta H(\Gamma)}}{\int d\Gamma \dot{x}\theta(\pm\dot{x})\delta(x)e^{-\beta H(\Gamma)}}. \quad (A.1)$$

Those trajectories with initial distribution $P^{(+)}(\Gamma)$ form the average of $P_+(t)$ while those with initial distribution $P^{(-)}(\Gamma)$ form the average of $P_-(t)$. Of course, for symmetric systems, $P_+(t) = P_-(t)$ and only one calculation is required. Initially the reaction coordinate x will be confined to the transition state $x = 0$ while the reaction coordinate velocity conforms to the weighted Gaussian distribution $\dot{x}e^{-\beta\dot{x}^2/2}$. The remaining, complementary coordinates will be distributed according to the Maxwell-Boltzmann distribution. The initial states are best generated by first calculating $P^{(+)}(\Gamma)$ and then simply reversing the velocities to produce $P^{(-)}(\Gamma)$ [15].

If the reaction coordinate is linear in Cartesian coordinates, the distribution for the position and velocity of the reaction coordinate may be separated from the position and velocity of the complementary coordinates[21]. This allows one to sample the initial state distribution $P^{(\pm)}(\Gamma)$ using the Box-Mueller sampling procedure as follows. The Gaussian random variate q_1 with probability distribution function $p(q_1) = e^{-q_1^2/2\sigma^2}$ is generated by[58]

$$q_1 = \left[-2\sigma^2 \log \varphi_1\right]^{\frac{1}{2}} \cos(2\pi\varphi_2) \quad (\text{A.2})$$

where φ_1 and φ_2 are random numbers uniformly distributed between zero and one and σ^2 is the variance of the sampled Gaussian distribution. Similarly, the random variate q_2 with weighted Gaussian probability distribution function $p(q_2) = q_2 e^{-q_2^2/2\sigma^2}$ is generated by[58]

$$q_2 = \left[-2\sigma^2 \log \varphi_1\right]^{\frac{1}{2}}. \quad (\text{A.3})$$

If the reaction coordinate is curvilinear, one cannot in general separate the reaction coordinate velocity from the positions of the complementary modes and the Monte Carlo sampling procedure should be used[17] where the probability distribution sampled is not the Maxwell-Boltzmann distribution, but the weighted distribution Eq. (A.1).

2) *Integrate the trajectories.* Check each step for crossing of the transition state. While very powerful integration algorithms exist, it has been shown that for most problems of interest in classical reaction dynamics, the velocity

version of the Verlet algorithm is the most efficient[21]. The algorithm is given below[102]

$$\begin{aligned}x_{n+1} &= x_n + hv_n + h^2 f(x_n)/2 \\v_{n+1} &= v_n + h[f(x_{n+1}) + f(x_n)]/2\end{aligned}\tag{A.4}$$

where x is the position, v is the velocity, $f(x)$ is the force divided by the mass of x , and h is the time step. The particular time step used will vary depending on the stiffness of the equations and the accuracy desired. However, for trajectory calculations it is best to start looking for a time step between 10^{-2} and 10^{-3} times the highest oscillation frequency in the system.

3) Calculate the survival probability $P_{\pm}(t)$ (or simply $P(t)$ for symmetric systems). Terminate the calculation after the survival probability is constant over an order of magnitude in time.

4) Extract the plateau values T_{\pm} (or simply T_o for symmetric systems). The transmission coefficient κ , the transition state normalized rate constant, is given simply as

$$\kappa = \frac{T_+ T_-}{T_+ + T_- - T_+ T_-} \quad \left(\text{or } \frac{T_o}{2 - T_o}\right).\tag{A.5}$$